Sound attenuation in a fully developed turbulent pipe flow

ter Horst, G.J.P.

Award date:
1992

Technische Universiteit Eindhoven

University of Technology
Den Dolech 2
P.O. Box 513
5600 MB Eindhoven, The Netherlands
Telephone: (040) 479111 Telex: 51163

Faculteit Technische Natuurkunde
Vakgroep Transportfysica

Titel:

SOUND ATTENUATION IN A FULLY DEVELOPED TURBULENT PIPE FLOW

Auteur: **G.J.P. ter Horst**

Verslagnummer: R-1167-A

Datum: **July 1992**

Werkeenheid: Gasdynamica/Aeroakoestiek (NT)

Begeleider(s): Dr. ir. A. Hirschberg
Ir. M.C.A.M. Peters
A.P.J. Wijnands
Dr. Ir. M.E.H. van Dongen

Dedicated to the women in my life: my wife and friend Esther and my daughter Marjolein.

Special thanks goes to all the people who have taken the time to discuss with me the contents of this report, and helped me whenever I needed that.

First of all, that is my direct supervisor, Mico Hirschberg, who has encouraged me to think further than my nose is long. Also, I'm indebted to Rene Peters, especially for his helpfull first comments on the script. The measurements could not have been made without the help and knowledge of our technician Bram Wijnands.

Also, I would like to thank Harm Jager, for his afternoon tea, and all the other people and fellow students of the department of transport physics, who made my time here pleasent and unforgetable, or, as they say in the netherlands, 'gezellig'.

Finally, I should thank the members of my graduation comitee, for spending their time to read my report, and the interest they showed for my work.

Summary

In this report, a theory based on a simple model of the apparent turbulent viscosity is used to describe the interactions of a fully developped turbulent pipe flow in hydraulicly smooth ducts with plane acoustical waves. This theory assumes a linear relationship between the apparent viscosity and the distance to the wall, with exception of a region very close to the wall, in which the turbulence vanishes. This region is called the laminar sub-layer, of which the thickness δ_l depends on the Reynolds number. Several limiting cases can be evaluated, resulting in different models of the apparent viscosity.

In the theory of Kirchhoff, describing the sound wave in the absence of flow, the attenuation is fully determined by the thickness of the acoustical boundary layer δ_v, which is a function of frequency.

The resulting attenuation in presence of a turbulent mean flow is therefore determined by the ratio δ_v/δ_l of the thickness of the two layers, and the Mach number, as a result of the Doppler effect. If the acoustical boundary layer is smaller than the laminar boundary layer, the attenuation will be determined by the Kirchhoff attenuation, shifted as result of the Doppler effect. On the other hand, if the acoustical boundary layer extends far into the turbulent zone, the attenuation will be determined by the thickness of the laminar sublayer, resulting in an almost constant attenuation, independent of frequency, and in our theory also independent of the Reynolds number. In the critical range of conditions, where $\delta_v \approx \delta_l$, some interference of the periodic acoustical shear wave (generated at the wall by the acoustiacl field) with it's reflection at the turbulent zone occurs. This interference results in an attenuation lower than the Kirchhoff estimate in the absence of mean flow.

These features of the theory are checked by measurements of the attenuation of plane acoustical waves in a duct with circular cross-section. A multiple microphone method is used to do this.

The measurements for high frequencies are well described by the theory, as was expected. The shift of up- and downstream attenuation, caused by the Doppler effect, is however larger than predicted by theory. A theory which includes only the effects on the attenuation due to the mean velocity profile, the quasi-laminar theory of Ronneberger [RON 77], predicts the measured shift very good, but doesn't describe the effect of turbulence itself.

The interference effect is also measured, but it's seems to be even stronger

than can be expected on basis of the assumption of total reflection of the shear wave at the edge of the laminar sub-layer, the so-called rigid plate model. Also, the value of the ratio δ_v/δ_l for which this minimum occurs, is not the same as predicted.

For low frequencies, the limiting value is also in good agreement with theory, showing no dependency on the Reynolds number within the measured range. For the models of the apparent viscosity similar to that used in describing the stationary turbulent flow, no modifications to the used dimensionless thickness of the laminar sublayer as found in stationary flow need to be made. The rigid plate model has to be evaluated using a different value for this quantity. The predicted doppler shift is in good agreement with measurement in this range.

We concluded that the theory correctly predicts the general features of the attenuation. Especially in the limiting cases, when one of the layer thicknesses δ_v or δ_l is much larger than the other. The model of the apparent viscosity which is identical to that used in describing stationary flow serves best to predict the resulting attenuations. This is of general importance, since the theory can than be expanded to include rough pipes by using the the same relation between the stationary flow properties and the acoustical disturbances, enlarging it's application range to many industrial situations.

Contents

0.1 introduction 5

1 Propagation of sound in a long pipe through a quiescent fluid. 8

1.1 Basic equations describing sound propagation in a quiescent fluid 9

1.2 Acoustical solution of the basic equations in case of a quiescent fluid. 11

1.3 Viscothermal attenuation of plane acoustical waves in a quiescent fluid. 13

1.4 Viscous and thermal acoustical boundary layers in a quiescent fluid. 16

1.5 Viscothermal attenuation of plane waves due to boundary layers in a quiescent fluid. 19

2 Propagation of sound in a long pipe with a turbulent mean flow 22

2.1 Basic equations governing the turbulent motions 23

2.2 Turbulent boundary layers due to a stationary mean flow . . . 26

2.3 Acoustical solution incorporating the effect of an axial mean flow. 31

2.4 acoustical boundary layer in case of a turbulent mean flow . . 33

2.5 Viscothermal attenuation of plane waves due to boundary layers in case of a turbulent mean flow. 42

2.5.1 Implications for measurement 44

3 Some other theories from literature 48

3.1 The stationary limit 49

3.2 The quasi-laminar limit 51

4 Measurement **52**
4.1 Experimental setup 53
4.2 Determination of the attenuation coefficient 56
4.3 Measurement results 60
4.3.1 measurement for the quiescent case 60
4.3.2 measurements with a turbulent mean flow 63

5 discussion **71**
5.1 Quiescent case 72
5.2 Situation with flow 72
5.2.1 The Kirchhoff limit 72
5.2.2 The dip 72
5.2.3 The static limit 77

6 Conclusions and recommendations **80**
6.1 Conclusions 81
6.2 recommendations 82

0.1 introduction

This report deals with theory and measurement of the propagation of plane pressure waves in long, hydraulicly smooth ducts, and especially the influence of a fully developed turbulent mean flow on the attenuation of those waves. This investigation is part of a project taking place at the laboratory of high velocities of the department of transport physics. This project on sound and vibration in pipe systems is supported by the N.V. Nederlandse Gasunie and FOM/STW, and subject of a doctoral study by Ir. M.C.A.M. Peters, under supervision of Dr. Ir. A. Hirschberg. The available theories and measurements in literature are not in agreement, and some of the basic principles are not well understood yet. In particular there is no universally accepted theory for turbulence in an unsteady flow. The main goal of this graduation research on sound attenuation, is to obtain a better insight in the general principles concerned.

Measurements of the attenuation are performed for various Mach numbers and frequencies. The pressure waves are created by a sirene, which can deliver a very strong wave. This high amplitude wave at discrete frequencies increases the quality of the measurement with respect to measurements using random noise. Also, the pressure wave doesn't have to be disturbed by entering the pipe with a pressure probe, as by the traversing probe method, because we measure the pressure at fixed positions with microphones placed in the wall of the tube. We call this the multiple microphone method.

The attenuation is thought to be mainly caused by interaction of acoustical viscothermal boundary layers at the wall of the pipe with the pressure waves. The effect of the turbulence on those boundary layers is in this report modelled by the introduction of a turbulent viscosity η_t in the equations for the mean flow. This turbulent viscosity represents the effect of the randomly fluctuating turbulent motions on the average motions. The equations for the average motions are obtained by time-averaging the equations for the total velocities, with a time-scale large enough to average out the turbulent fluctuations, but yet so small that the periodical fluctuations with radial frequencies ω we want to investigate (sound) are maintained in the equations for the mean quantities.

In theories on sound attenuation in pipes without mean flow, the main parameter is the thickness of the viscous (acoustical) boundary layer $\delta_v =$

$\sqrt{2\eta/\rho_0\omega}$, with η the dynamic viscosity and ρ_0 the mean density. In our case we will only look at experimental conditions for which this thickness is much smaller than the radius of the pipe a, so we neglect influence of the radius of the pipe on the boundary layer. We will also confine ourselves to waves with wavelengths $\lambda = c_0/f$ much longer than the radius of the pipe, so only plane waves can propagate. Another parameter is the Mach number $M = U_0/c_0$, the ratio of the mean flow velocity U_0 and the speed of sound for a quiescent fluid c_0, which affects the speed of sound relative to the wall in the up- and downstream direction ($c = c_0 \pm U_0$). It's influence on the attenuation is a shift between the up- and downstream attenuation. Since we've measured with only one pipe, with fixed radius a, and one fluid with fixed mean density (air under atmospheric conditions), the Mach number $M = U_0/c_0$ and the Reynolds number $Re = 2U_0a\rho_0/\eta$ are directly connected.

The effect of an apparent turbulent viscosity η_t in turbulent flow on the mean flow quantities in the absence of sound is the division of the velocity profile in two regions. A laminar region near the wall of a certain thickness δ_l, in which no turbulence exists, and a turbulent region for the main part of the flow. For the description of this steady turbulent flow, the thickness of the laminar sublayer δ_l turns out to be a major parameter. In our theory for the turbulent viscosity, we assumed also that the thickness of this laminar layer is much smaller than the radius of the pipe. In the determination of the relation between this thickness and the mean pipe flow, we used the radius of the pipe, introducing a dependency on the Reynolds number Re. The theory used is only valid low Mach number flows ($M \ll 1$), because we neglect the effect of stationary dissipation on the temperature and pressure distribution in the flow.

The interaction of sound in case of a turbulent mean flow will in first instance be governed by the ratio of δ_v/δ_l. For small values of this ratio, the entire viscous boundary layer will be within the laminar sublayer, where only the dynamic viscosity η determines the shape of the boundary layer. The attenuation will therefore behave similar to that in the quiescent case, depending only on δ_v, altered for the up- and downstream direction according the Mach number.

For large values of this ratio, the viscous boundary layer will be mainly in the turbulent region, where it is controlled by the apparent turbulent viscosity, causing a drastic increase of the attenuation. The viscous boundary

layer will be governed by the thickness of the laminar boundary layer δ_l, corresponding to a quasi-steady limit of the acousic flow behaviour. The Mach number again is responsible for a shift for the up- and downstream attenuation.

Since this apparant viscosity η_t is able to describe the structure of steady turbulent pipe flow quite satisfactory, it's basic features might be able to describe the change in the acoustical boundary layers due to the turbulence as well. This is of great practical importance, since the theory of turbulent boundary layers is then directly related to the attenuation of plane pressure waves. This means, that the theory of attenuation can be extended to incorporate the effect of rough walls by using the same relation between the steady flow properties and the acoustical disturbances.

Worth mentioning is the situation of closed side branches in complex pipe systems, as in the gas industry. Those side-branches can generate low-frequency acoustical disturbances, or even high amplitude standing waves. In calculating the resulting amplitudes, the attenuation plays an important role. For this reason, the N.V. Nederlandse Gasunie is interested in our research.

Also, at TNO-TPD in Delft, they have developed a program to do these kind of calculations, called PULSIM. It is used as a development tool for designing complex pipe systems. An accurate description of sound attenuation can of course contribute to the quality of the calculations, and the final design.

Another interesting application is the measurement of mean flow velocities by measuring the amplitude ratio of standing waves [SHA 91]. Knowledge about the attenuation is important, since the accuracy of such measurements depends strongly on the (difference in) phase velocity of the sound wave in the up- and downstream direction. This phase velocity is influenced by the turbulent interactions.

A medical application we refer to, is the measurement of the radiation and entry impedance of the respiratory system. It turns out that the interaction of turbulence with the oscillating flow is important in determining these physiologically important quantities. An investigation on this subject was made by Louis and Isabey [LOU 92].

Chapter 1

Propagation of sound in a long pipe through a quiescent fluid.

Much of what is written in this chapter can also be found in textbooks on acoustics, such as 'Acoustics' of Allan D. Pierce [PIE 89], and 'Waves in fluids', from Sir James Lighthill [LIG 80]. Sometimes, results obtained in these textbooks are presented as facts, since the underlying theories are beyond the scope of this report. The reader will then be referred to these textbooks.

1.1 Basic equations describing sound propagation in a quiescent fluid

To obtain a description of the propagation of acoustical waves in a quiescent fluid in a pipe, the well known equations of conservation of mass, momentum and energy will be used as starting point. These equations will be completed with constitutive equations and thermodynamic relations between the acoustical quantities, assuming local thermodynamic equilibrium.

When considering only small deviations from an uniform and stationary state, the behaviour of the physical quantities can be linearised by writing a quantity Q as:

$$Q = Q_0 + Q' \quad \text{where: } \frac{Q'}{Q_0} << 1$$

and since we're considering a quiescent state in which $\vec{v_0} = 0$

$$\vec{v} = \vec{v'} \quad \text{where: } \frac{|\vec{v'}|}{c_0} << 1 \tag{1.1}$$

a limit which is essentially imposed by the condition that $\rho'/\rho_0 \ll 1$, a necessary condition for the validity of the linearization of the thermodynamic relations. Furthermore the thermal conductivity κ and the viscosity η of the Newtonian fluid will be considered as uniform and constant. These assumptions yield the following set of *linearised equations.*
Mass conservation:

$$\frac{\partial \rho'}{\partial t} + \rho_0 \vec{\nabla} \cdot \vec{v'} = 0 \tag{1.2}$$

momentum conservation (linearised Navier-Stokes equation):

$$\rho_0 \frac{\partial \vec{v'}}{\partial t} = -\vec{\nabla} p' + \eta[\nabla^2 \vec{v'} + \frac{1}{3}\vec{\nabla}(\vec{\nabla} \cdot \vec{v'})] \tag{1.3}$$

and energy conservation:

$$\rho_0 T_0 \frac{\partial s'}{\partial t} = \kappa \nabla^2 T' \tag{1.4}$$

And the thermodynamic relations, which are added to obtain a complete set of equations:

$$\rho' = \frac{1}{c_0^2} p' - \frac{\rho_0 \beta T_0}{c_p} s' \tag{1.5}$$

$$T' = \frac{T_0 \beta}{\rho_0 c_p} p' + \frac{T_0}{c_p} s' \tag{1.6}$$

in which the definitions for the adiabatical speed of sound $c_0^2 = \frac{\partial p}{\partial \rho}\Big|_S$, the specific heat at constant pressure $c_p = T \frac{\partial s}{\partial T}\Big|_P$, and the coefficient of thermal expansion $\beta = \rho \frac{\partial 1/\rho}{\partial T}\Big|_P$ are used.

These are the basic equations used in describing the propagation of small perturbations of an ambient state in a quiescent fluid, called sound.

In the following sections, the propagation of sound in a long pipe will be described, neglecting the effects of thermal conduction and viscosity. The only boundary condition is then, that the velocity at the wall is parallel to that wall (the fluid can't penetrate the wall). Also an estimate will be given of the attenuation as a result of viscous and thermal dissipation.

Next, the effects of viscosity and heat conduction near the wall will be taken into account, which results for sufficiently high frequencies in a boundary layer description for the acoustic velocity and temperature.

Finally, the results will be combined to determine the complex attenuation of the sound waves propagating along the axis of the pipe.

1.2 Acoustical solution of the basic equations in a pipe filled with a quiescent fluid.

The goal is to derive an equation describing the propagation of sound in a long pipe. The thermal conductivity κ and the viscosity η are in first approximation set to zero, since the effect on the propagation is expected to be small. The conditions determining the validity of this approximation will be discussed in section 1.3, when the effects of visco-thermal dissipation are estimated. In doing so, the basic equations reduce to:

$$\frac{\partial \rho'}{\partial t} + \rho_0 \vec{\nabla} \cdot \vec{v}' = 0 \tag{1.7}$$

$$\rho_0 \frac{\partial \vec{v}'}{\partial t} = -\vec{\nabla} p' \tag{1.8}$$

$$\frac{\partial s'}{\partial t} = 0 \tag{1.9}$$

and for the thermodynamic relations, in which we have used (1.9):

$$\rho' = \frac{1}{c_0^2} p' \tag{1.10}$$

$$T' = \frac{T_0 \beta}{\rho_0 c_p} p' \tag{1.11}$$

As long as confusion with the other quantities is unlikely, the primes will be omitted in the rest of this paper.

To get an equation for p, (1.10) is used to eliminate ρ by p in equation (1.7). Taking the time derivative of the result gives:

$$\frac{1}{c_0^2} \frac{\partial^2 p}{\partial t^2} + \rho_0 \vec{\nabla} \cdot \frac{\partial \vec{v}}{\partial t} = 0$$

Together with the divergence of Euler's equation (1.8):

$$\rho_0 \vec{\nabla} \cdot \frac{\partial \vec{v}}{\partial t} = -\nabla^2 p$$

and after elimination of the factor $\rho_0 \vec{\nabla} \cdot \partial \vec{v} / \partial t$, we come to the wave-equation for the pressure disturbance p:

$$\frac{1}{c_0^2} \frac{\partial^2 p}{\partial t^2} = \nabla^2 p \tag{1.12}$$

This equation, the Helmholz equation, can be solved analytically for certain boundary conditions. In the case of a pipe with radius a, for radial frequencies $\omega = 2\pi f$ below the so-called cutoff frequency ω_{cutoff}, the only propagating solution is a plane wave along the axis of the pipe (x-axis), with no dependency on the radial and azimuthal coordinates. All the other solutions die out within a length of order $\lambda = c_0/f$ [KON 91]. This cutoff frequency for cylindrical pipes is given by [PIE 89]:

$$\omega_{cutoff} = 1.841 \frac{c_0}{a} \tag{1.13}$$

So the acoustical solution for a pipe of small radius $a < \lambda/\pi$ is given by:

$$p = \hat{p} e^{\, i(kx - \omega t)} \tag{1.14}$$

$$k^2 = \frac{\omega^2}{c_0^2} \tag{1.15}$$

in which the dispersion relation (1.15) has been obtained by substituting (1.14) in (1.12). The final result for the pressure p is:

$$p = \Re[\, \hat{p}^+ e^{\, i(k_0 x - \omega t)} + \hat{p}^- e^{\, i(-k_0 x - \omega t)} \,] \tag{1.16}$$

$$\text{with: } k_0 = \frac{\omega}{c_0} \tag{1.17}$$

where $\hat{p}^+$ and $\hat{p}^-$ are the complex amplitudes of the waves travelling in the positive and negative direction. From (1.17) a similar equation for the other acoustical quantities can be derived, because they are all linearly related to p. The relation between the pressure p and the velocity $\vec{v}$ i.e. is:

$$\hat{u}^\pm = \frac{k\hat{p}^\pm}{\omega \rho_0} = \pm \frac{\hat{p}^\pm}{\rho_0 c_0} \tag{1.18}$$

In having derived a solution for the acoustical quantities, a check should be made on the validity of the initial assumptions. This check will be made in the next section, where the attenuation as a result of the viscous and thermal terms, is calculated.

1.3 Viscothermal attenuation of plane acoustical waves in a quiescent fluid.

In order to estimate the attenuation of sound in the absence of walls, but with thermal and viscous dissipation, *the relations found in the previous section for the acoustical quantities are used to estimate the order of magnitude of the terms involving viscous dissipation and heat conduction, which have been neglected.*The resulting error in the estimate of these terms will be small if the attenuation is small compared to the wavenumber. These terms involve the change in density due to the entropy change, as given in (1.5), and the last term in the equation of momentum conservation (1.3), representing the shear stresses due to the viscosity.

So, the relation between the temperature fluctuation T_{ac} and the pressure p_{ac} (1.11), derived in the previous section, is substituted into the energy equation incorporating the effect of heat conduction (1.4), to give an estimate of the entropy change $\partial s/\partial t$ in terms of p.

$$\frac{\partial s}{\partial t} = \frac{\kappa}{\rho_0 T_0}\frac{\partial^2 T}{\partial x^2} = \frac{\kappa\beta}{\rho_0^2 c_p}\frac{\partial^2 p}{\partial x^2} \tag{1.19}$$

Then, the density fluctuations $\partial\rho/\partial t$ can be calculated using (1.5), resulting in

$$\frac{\partial \rho}{\partial t} = \frac{1}{c_0^2}\frac{\partial p}{\partial t} - \frac{\kappa\beta^2 T_0}{\rho_0 c_p^2}\frac{\partial^2 p}{\partial x^2} \tag{1.20}$$

This yields the following equations for the conservation of mass (1.2) and momentum (1.3):

$$\frac{1}{c_0^2}\frac{\partial p}{\partial t} - \frac{\kappa(\gamma-1)}{c_0^2\rho_0 c_p}\frac{\partial^2 p}{\partial x^2} + \rho_0\frac{\partial u}{\partial x} = 0 \tag{1.21}$$

$$\rho_0\frac{\partial u}{\partial t} = -\frac{\partial p}{\partial x} + \frac{4\eta}{3}\frac{\partial^2 u}{\partial x^2} \tag{1.22}$$

The thermodynamic identity $\gamma - 1 = T_0\beta^2 c_0^2/c_p$ is used to rewrite the second term on the left of equation (1.21) [PIE 89].

If we assume again that only plane waves will propagate, we can solve these two equations for u and p. Instead of using this exact solution, we will

use the approximate linear relation between u and p (1.18), derived in the previous section to rewrite the last term on the right-hand side. Then we can eliminate u by the same procedure as in the previous section. The resulting homogeneous relation for p then becomes for harmonic waves $e^{\,i(k_{vt}x - \omega t)}$:

$$k_{vt}^2 p = \left(\frac{\omega^2}{c_0^2} + i\frac{\omega k_{vt}^2 \kappa(\gamma - 1)}{c_0^2 \rho_0 c_p} + i\frac{4k_{vt}^4 \eta}{3\omega\rho_0}\right) p \tag{1.23}$$

giving us the following dispersion relation:

$$k_{vt}^2 \approx \frac{\omega^2}{c_0^2}\left[1 + \frac{i\omega\eta}{c_0^2\rho_0}\left(\frac{4}{3} + \frac{\gamma - 1}{Pr}\right)\right] \tag{1.24}$$

with $Pr = \eta c_p/\kappa$. The change of k due to introduction of the effects of viscosity and heat conduction will be small, and therefore, to first order, k_{vt} is approximated by ω/c_0, whenever product terms involving small quantities are considered. This, and using the taylor expansion $(1 + x)^{1/2} \approx 1 + x/2$, determines the wavenumber k:

$$k_{vt} = \pm\frac{\omega}{c_0} \pm i\frac{\omega^2\eta}{2c_0^3\rho_0}\left(\frac{4}{3} + \frac{\gamma - 1}{Pr}\right) = \pm k_0 \pm i\alpha_{vt} \tag{1.25}$$

We see that the result for k is an additional imaginairy part $i\alpha_{vt}$. By writing the pressure wave as follows, we see that α_{vt} describes the amplitude attenuation.

$$p = \Re\left[\hat{p}^+ e^{\,-\alpha_{vt}x} e^{\,i(k_0 x - \omega t)} + \hat{p}^- e^{\,\alpha_{vt}x} e^{\,i(-k_0 x - \omega t)}\right] \tag{1.26}$$

We can now estimate the error made by neglecting the viscosity and heat conduction by looking at equation (1.24). We can substract the relation from it that must be fullfilled if the theory is to be valid. This relation is:

$$\frac{\omega\eta}{c_0^2\rho_0}\left(\frac{4}{3} + \frac{\gamma - 1}{Pr}\right) \ll 1 \tag{1.27}$$

When using the values for air, we come to a maximum radial frequency ω of:

$$\omega \ll 4 \cdot 10^9 Hz \tag{1.28}$$

It is then clear that the attenuation described by the imaginary part of k_{vt} is only a minor part of the magnitude $|k_{vt}|$ of the wavenumber, so that the

assumption that viscosity and heat conduction are only a small effect, and therefore of minor influence on the propagation, is justified. It must be mentioned, that the actual attenuation can increase strongly even below this limit, because of the departure from local thermodynamic equilibrium. We have ignored this effect here.

1.4 Viscous and thermal acoustical boundary layers in a quiescent fluid.

In the previous sections the consequences of viscosity and heat conduction near a wall have not been considered, we only discussed bulk attenuation. The boundary conditions alter significantly when taking these wall effects into account. The viscosity requires the velocity at the wall to be zero, while for the heat conduction we will assume that the temperature variations become zero at the wall, because $(\kappa\rho c_p)_{wall} \gg (\kappa\rho_0 c_p)_{fluid}$ [PIE 89]. In order to achieve these boundary conditions, a thin boundary layer is formed. This means that the velocity u and temperature T, which until now were only a function of the axial coordinate x, will in a region close to the wall also be a function of the radial coordinate r.

Since the variations of the acoustical quantities with the radial coordinate take place over a distance, say δ, which is much shorter than the wavelength λ, over which the same variations occur in the axial direction, all terms containing a derivative in the axial direction of a quantity can be neglected in comparison with terms containing a radial derivative of that quantity. Also, when the radius a of the pipe is large, compared to the thickness δ of the boundary layer, the equations reduce to those for a two-dimensional flow along a boundary in the x, y-plane. Since the boundary, the x-axis, is a straigth line, the flow will be assumed parallel, neglecting the radial velocity v of order $u\delta/\lambda$, as can be derived from the law of mass conservation. So we assume $\vec{v} = (u(y), 0)$. This reduces the Navier-Stokes equation for the y-direction normall to the wall to:

$$\frac{\partial p}{\partial y} = 0 \tag{1.29}$$

resulting in a pressure, uniform over the cross-section of the pipe.

Neglecting the terms proportional to δ/λ in the Navier-Stokes equation, we get for the axial x-direction:

$$\rho_0 \frac{\partial u}{\partial t} = -\frac{\partial p_{ac}}{\partial x} + \eta \frac{\partial^2 u}{\partial y^2} \tag{1.30}$$

$$u|_{y=0} = 0 \text{ (boundary condition)} \tag{1.31}$$

in which the pressure gradient $\partial p_{ac}/\partial x$ is the driving force for the flow. The particular $\hat{u}_p$ and general $\hat{u}_g$ solutions to this problem for harmonic waves,

are given in complex notation by

$$\hat{u}_p = \frac{\partial \hat{p}_{ac}}{\partial x}\frac{1}{\rho_0 i\omega_{ac}} \tag{1.32}$$

$$\hat{u}_g = \hat{u}_1 e^{-\epsilon_v y} + \hat{u}_2 e^{\epsilon_v y} \tag{1.33}$$

$$\epsilon_v = \sqrt{\frac{-i\omega_{ac}\rho_0}{\eta}} = (1-i)\sqrt{\frac{\omega_{ac}\rho_0}{2\eta}} \tag{1.34}$$

Subjecting this solution to the boundary condition, considering the solution being finite for $y \to \infty$, which is essentially the same as imposing the second boundary condition to be

$$u|_{y\to\infty} = u_{ac} \text{ (boundary condition)} \tag{1.35}$$

gives the velocity profile in the pipe:

$$\hat{u} = \frac{\partial \hat{p}_{ac}}{\partial x}\frac{1}{\rho_0 i\omega_{ac}}(1 - e^{-\epsilon_v y}) \tag{1.36}$$

$$u = u_{ac}(1 - e^{-\epsilon_v y}) = u_{ac} + u_{bl} \tag{1.37}$$

The deviation $u_{bl} = -u_{ac}e^{-\epsilon_v y}$ from the plane-wave velocity u_{ac} describes an attenuated wave propagating in the y-direction, the so-called shear wave (fig. 1.1). We can define de distance over which the amplitude of the wave decreases a factor e as the thickness δ_v of the viscous boundary layer. So,

$$\delta_v = \sqrt{\frac{2\eta}{\omega_{ac}\rho_0}} \tag{1.38}$$

Similarly, the thermal boundary layer is described by the energy equation (1.4), completed with the thermodynamic relation (1.6) for the temperature T:

$$\rho_0 c_p \frac{\partial}{\partial t}\left(T - \frac{T_0\beta}{\rho_0 c_p}p_{ac}\right) = \kappa\frac{\partial^2 T}{\partial y^2} \tag{1.39}$$

$$T|_{y=0} = 0 \text{ (boundary condition)} \tag{1.40}$$

The solution is now:

$$T = \frac{T_0\beta}{\rho_0 c_p}p_{ac}(1 - e^{-\epsilon_T y}) = T_{ac}(1 - e^{-\epsilon_T y}) = T_{ac} + T_{bl} \tag{1.41}$$

$$\epsilon_T = \sqrt{\frac{-i\omega\rho_0 c_p}{\kappa}} = (1-i)\sqrt{\frac{\omega\rho_0 c_p}{2\kappa}} \tag{1.42}$$

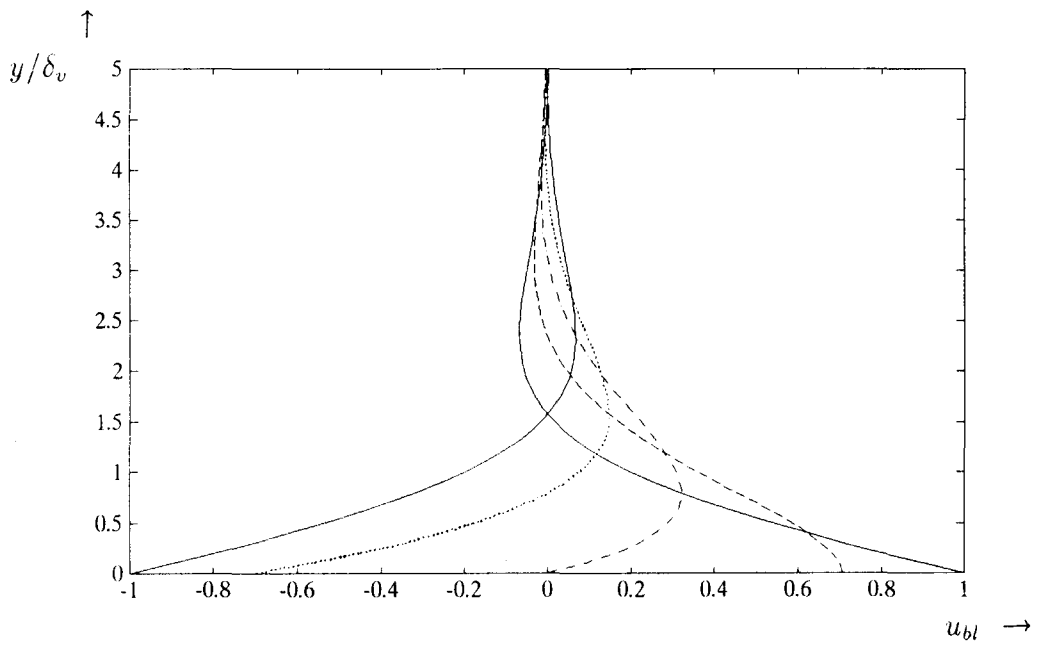

Figure 1.1: The shear wave, u_{bl} as function of y/δ_v.
—— $\omega t = 0$; - - - $\omega t = \pi/4$; · − · − · $\omega t = 2\pi/4$; · · · $\omega t = 3\pi/4$; —— $\omega t = \pi$

For gases $Pr = \eta/\kappa c_p = O(1)$, so that the thermal and viscous boundary layers will have a comparable thickness δ. We can now check the validity of the assumption that the boundary layer thickness is small compared to the radius of the pipe $\delta \ll a$. We have:

$$\delta = \sqrt{\frac{2\eta}{\omega\rho_0}} \ll a \tag{1.43}$$

$$\omega \gg 0.1 \ rad \ s^{-1} \tag{1.44}$$

$$\text{for: } a = 0.015 \ m \tag{1.45}$$

where weve used the diameter of the pipe we've used for our measurements. Note that because we assume plane waves, so that $a < \lambda$, we automatically satisfy the condition $\delta \ll \lambda$, which we have used in the derivation of our equations.

The two profiles obtained by this procedure satisfy the boundary conditions imposed by the viscosity and heat conduction, while for $y \to \infty$ they asymptoticaly approach the solutions found when neglecting the influence of the wall. Also, the thickness of the boundary layers found is small, compared to both the wavelength λ and the radius a of the pipe, as assumed. These are the kind of solutions we were looking for.

1.5 Viscothermal attenuation of plane waves due to boundary layers in a quiescent fluid.

In the previous section expressions have been obtained describing the velocity and temperature distribution near the wall, in the viscous and thermal boundary layers, that fullfill the boundary conditions imposed by the viscosity and thermal conductivity. In order to estimate the effect of these boundary layers on the propagation of the acoustical waves, the procedure used in the previous sections to derive a dispersion relation determining the wave number k must be modified, since the acoustical quantities are no longer uniform over the cross-section of the pipe. Therefore, the terms in the mass and momentum conservation laws containing acoustical quantities are averaged by integrating these terms over the cross-section.

For the terms involving quantities still uniform, such as p, the integration results in multiplication by the cross-sectional area $\mathcal{A}$.

For the terms involving non-uniform quantities, such as $T = T_{ac} + T_{bl}$ and $u = u_{ac} + u_{bl}$, the integration is performed in two parts. The uniform (acoustical) part is treated as above, whereas the non-uniform boundary-layer part is integrated over the normal coordinate y and multiplied by the perimeter of the cross-section $\mathcal{L}$. The integration over the normal coordinate y is mathematically taken from zero to ∞, which is allowed since the integrand vanishes for $y \gg \delta_v$, δ_T. We will write however as upper limit the thickness of the boundary layer, to emphasise that the contribution of the boundary layer for $y > \delta$ is negligable. [HOW 79] [PIE 89]

This division of the integration in two parts is not as obvious as it seems, because we must recall that the *boundary layer*solutions were found by solving simplified boundary layer equations for mass, momentum and energy conservation,*including the effects of viscosity and heat transport*, whereas the *acoustical solutions*were found by*neglecting thermoviscous effects.*Therefore, to be consistent, the thermal and viscous terms are only taken into account for the boundary layer contributions u_{bl} and T_{bl}, and are neglected for the uniform contributions of these quantities u_{ac} and T_{ac}. This is the same as stating that we will neglect any terms involving the viscothermal attenuation found in section 1.3, assuming that they result in only a minor contribution to the total attenuation. The equations of conservation of mass and momentum

are then given by:

$$\frac{1}{c_0^2}\frac{\partial p}{\partial t} + \frac{\kappa\beta}{c_p}\frac{\partial^2 T_{bl}}{\partial y^2} + \rho_0\frac{\partial u}{\partial x} = 0 \tag{1.46}$$

$$\rho_0\frac{\partial u}{\partial t} = -\frac{\partial p}{\partial x} + \eta\frac{\partial^2 u_{bl}}{\partial y^2} \tag{1.47}$$

After integration over the cross-section, this results in the following equations:

$$\mathcal{A}\left(\frac{1}{c_0^2}\frac{\partial p}{\partial t} + \rho_0\frac{\partial u_{ac}}{\partial x}\right) + \mathcal{L}\left(\rho_0\frac{\partial}{\partial x}\int_0^{\delta_v} u_{bl}dy - \frac{\kappa\beta}{c_p}\int_0^{\delta_T}\frac{\partial^2 T_{bl}}{\partial y^2}dy\right) = 0$$

$$\mathcal{A}\rho_0\frac{\partial u_{ac}}{\partial t} + \mathcal{L}\rho_0\frac{\partial}{\partial t}\int_0^{\delta_v} u_{bl}dy = -\mathcal{A}\frac{\partial p}{\partial x} + \mathcal{L}\eta\int_0^{\delta_v}\frac{\partial^2 u_{bl}}{\partial y^2}dy$$

Performing the second step of the choosen procedure, the elimination of the acoustical velocity u_{ac}, results in:

$$\frac{1}{c_0^2}\frac{\partial^2 p}{\partial t^2} - \frac{\partial^2 p}{\partial x^2} = \frac{\mathcal{L}}{\mathcal{A}}\left[-\eta\frac{\partial}{\partial x}\int_0^{\delta_v}\frac{\partial^2 u_{bl}}{\partial y^2}dy + \frac{\kappa\beta}{c_p}\frac{\partial}{\partial t}\int_0^{\delta_T}\left(\frac{\partial^2 T_{bl}}{\partial y^2}\right)dy\right] \tag{1.48}$$

The integrals can be evaluated, when realising that $\partial Q_{bl}/\partial y = 0$ for $y \to \infty$. So:

$$\int_0^{\delta}\frac{\partial^2 Q_{bl}}{\partial y^2}dy = -\left(\left.\frac{\partial Q_{bl}}{\partial y}\right|_{y=\delta} - \left.\frac{\partial Q_{bl}}{\partial y}\right|_{y=0}\right) = \left.\frac{\partial Q_{bl}}{\partial y}\right|_{y=0} \tag{1.49}$$

The minus sign is a result of the definition of y, being the normal coordinate*pointing in the direction of the centre of the pipe.* This finally leads us to the dispersion relation for harmonic waves of the form $e^{\,i(\pm k_{bl\pm}x - \omega t)}$:

$$-\frac{\omega^2}{c_0^2}\hat{p}_{ac} + k_{bl}^2\hat{p}_{ac} = \frac{\mathcal{L}}{\mathcal{A}}\left[ik_{bl}\eta\left.\frac{\partial\hat{u}_{bl}}{\partial y}\right|_{y=0} + \frac{i\omega\kappa\beta}{c_p}\left.\frac{\partial\hat{T}_{bl}}{\partial y}\right|_{y=0}\right] \tag{1.50}$$

which, for a circular pipe with radius a, under the same assumptions as in section 1.3, results in:

$$k_{bl\pm} = \pm k_0 \pm \frac{1}{2ac_0}\left[(1+i)\sqrt{\frac{2\omega\eta}{\rho_0}}\left(1 + \frac{\gamma-1}{\sqrt{Pr}}\right)\right] \tag{1.51}$$

$$= \pm k_0 \pm (1+i)\alpha_0 \tag{1.52}$$

$$\text{with: } \alpha_0 = \left(1 + \frac{\gamma - 1}{\sqrt{Pr}}\right)\alpha_v \tag{1.53}$$

$$\tag{1.54}$$

$$\text{and: } \alpha_v = \frac{1}{2ac_0}\sqrt{\frac{2\omega\eta}{\rho_0}} \tag{1.55}$$

The attenuation due to the viscothermal effects near the wall of the pipe appears to be much larger than the attenuation due to dissipation and heat transfer in the bulk of the fluid. The maximum radial frequency for which the effect of this bulk attenuation is negligible, is given by the following relation:

$$\frac{\alpha_{vt}}{\alpha_0} \approx \frac{\omega^2\eta}{2c_0^2\rho_0}\sqrt{\frac{\rho_0}{2\omega\eta}} = \sqrt{\frac{\omega^3\eta}{8c_0^4\rho_0}} \ll 1 \tag{1.56}$$

$$\omega \ll 2 \cdot 10^5 rads^{-1} \tag{1.57}$$

The attenuation due to the boundary layers results in a change of the apparent phase velocity $c_{ph} = \omega/\Re(k)$ of the sound wave, an effect not seen in the free-space attenuation according to equation (1.25) [PIE 89]. Equation (1.25) is however not exact, and a small decrease in the phase velocity is observed for low frequencies, due to the change from adiabatic to isothermal sound propagation. This effect is however small compared to the effect considered here.

Knowledge about the fundamental structure of the boundary layers is of the utmost importance when trying to calculate the sound attenuation in ducts. Especially when the propagation of sound through a pipe with a turbulent mean flow is to be examined, the interaction of the boundary layers with the mean flow must carefully be incorporated in the description of the acoustical quantities. An attempt to describe these interactions is made in the next chapter.

Chapter 2

Propagation of sound in a long pipe with a turbulent mean flow

Just as the previous section, this section is based on theories described in many textbooks. Especially 'Boundary layer theory', written by Schlichting [SCH 79], and 'Turbulence' by Hinze [HIN 75], are often quoted. The reader is again referred to this textbooks for additional information.

The basic idea of the theory described is based on two papers, written by Howe [HOW 79] [HOW 84]. These can be very helpfull when studying this chapter.

2.1 Basic equations governing the turbulent motions

In order to obtain a description of the acoustical boundary layer in the case of a turbulent mean flow trough a pipe, first the structure of the turbulent mean flow in the absence of sound is examined. A well-known procedure is used, to calculate the effect of the turbulent motion on the flow. We start by seperating the physical quantities into two parts. One part being the mean quantity $\overline{Q}$, and the other part the randomly fluctuating part $\tilde{Q}$:

$$Q = \overline{Q} + \tilde{Q} \tag{2.1}$$

This decomposition is then substituted in the incompressible Navier-Stokes equation

$$\rho_0 \frac{\partial \vec{v}}{\partial t} + \rho_0 (\vec{v} \cdot \vec{\nabla}) \vec{v} = -\vec{\nabla} p + \vec{\nabla} \cdot \eta \vec{\vec{D}} \tag{2.2}$$

$$\vec{\vec{D}} = \begin{pmatrix} 2\frac{\partial u}{\partial x} & \frac{\partial u}{\partial y} + \frac{\partial v}{\partial x} & \frac{\partial u}{\partial z} + \frac{\partial w}{\partial x} \\ \frac{\partial v}{\partial x} + \frac{\partial u}{\partial y} & 2\frac{\partial v}{\partial y} & \frac{\partial v}{\partial z} + \frac{\partial w}{\partial y} \\ \frac{\partial w}{\partial x} + \frac{\partial u}{\partial z} & \frac{\partial w}{\partial y} + \frac{\partial v}{\partial z} & 2\frac{\partial w}{\partial z} \end{pmatrix} \tag{2.3}$$

which is then averaged over a time t_{av}, long enough to average out the turbulent fluctuations. Variations in the mean quantities still can exist over periods much longer than the averaging period. The condition of incompressibility will be satisfied if the Machnumber $M \ll 1$, see [SCH 79].

The result is the familiar Navier-Stokes equation for the mean quantities, altered by a term containing the averaged products of the turbulent velocities $\tilde{u}$, $\tilde{v}$ and $\tilde{w}$:

$$\rho_0 \frac{\partial \overline{\vec{v}}}{\partial t} + \rho_0 (\overline{\vec{v}} \cdot \vec{\nabla}) \overline{\vec{v}} = -\vec{\nabla} \overline{p} + \vec{\nabla} \cdot 2\eta \overline{\vec{\vec{D}}} + \vec{\nabla} \cdot \vec{\vec{S}}_r \tag{2.4}$$

$$\vec{\vec{S}}_r = -\rho_0 \begin{pmatrix} \overline{\tilde{u}^2} & \overline{\tilde{u}\tilde{v}} & \overline{\tilde{u}\tilde{w}} \\ \overline{\tilde{v}\tilde{u}} & \overline{\tilde{v}^2} & \overline{\tilde{v}\tilde{w}} \\ \overline{\tilde{w}\tilde{u}} & \overline{\tilde{w}\tilde{v}} & \overline{\tilde{w}^2} \end{pmatrix} \tag{2.5}$$

$\vec{\vec{S}}_r$ is called Reynolds stress tensor, for he was the first to formulate the above equations. The precise form of $\vec{\vec{S}}_r$ is not known, but the following argumentation can give some insight in the properties of the Reynolds stress tensor. It is a short version of an argumentation held in the book 'Boundary layer theory', by Schlichting [SCH 79]. It is strongly recommended to read the original version, since it is a more complete argumentation.

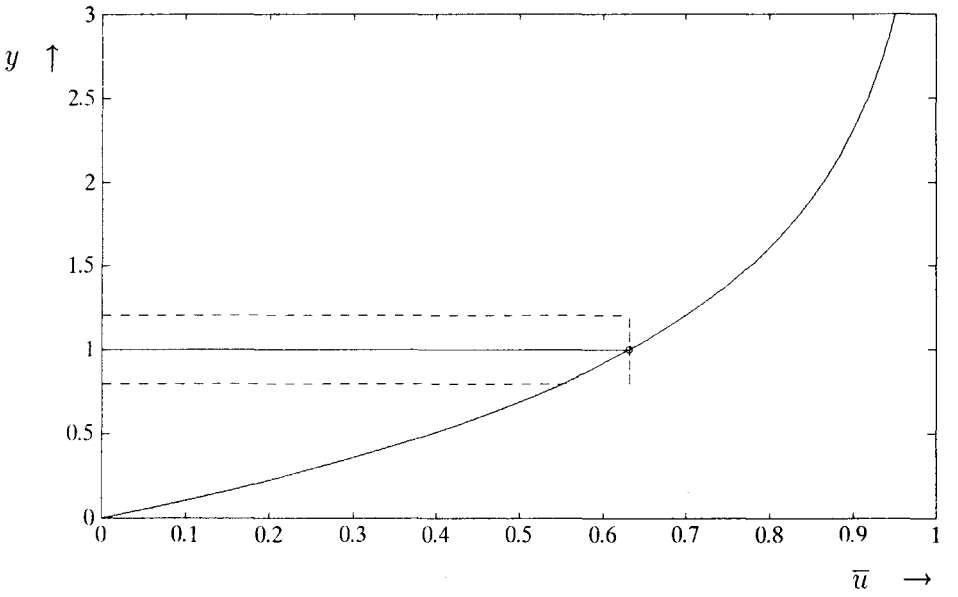

Figure 2.1: The turbulent shearing motion $\overline{u}$ (horizontal axis) as function of y (vertical axis).
$\cdots$ velocity difference.

That the time averages, like $\overline{\tilde{u}\tilde{v}}$, differ from zero, can be argued by considering a hypothetical two-dimensional shear flow, as in figure (2.1). When fluid particles with a turbulent velocity of $+\tilde{v}$ move from y_0 upwards, they arive at a lamina in which a higher mean velocity $\overline{u}$ prevails. The mean velocity deficient occuring, will generally give rise to a lower longitudinal turbulent velocity in the lamina at y_{+l}. Conversely, particles which move downwards due to a turbulent velocity $-\tilde{v}$, will generally give rise to an in-

crease in the turbulent velocity $\tilde{u}$ at y_{-l}. So, mostly, $\tilde{u}$ is associated with $-\tilde{v}$, and therefore the turbulent stress $\overline{\tilde{u}\tilde{v}}$ will be negative. It is easily seen, that to first order, a fluid particle coming from a lamina a distance l away, will introduce a turbulent velocity $\tilde{u}$ of approximately $l\partial\overline{u}/\partial y$.

The magnitude of the transverse turbulent velocity $\tilde{v}$ will be of the same order of magnitude, by considering the mechanism by which they are generated. Consider two particles ariving at a lamina a distance y_0 from the wall, the slower one from y_{-l} preceding the faster one from y_{+l}. These particles will collide, and thereby squeeze out the fluid separating them, and in doing so introduce a transverse velocity. Similar, if the faster particle preceeds the slower one, the growing space between them will be filled in by the surrounding fluid, again giving rise to a transverse velocity.

Consequently, the total average Reynold stress can be written as

$$-\rho_0\overline{\tilde{u}\tilde{v}} = \rho_0 l^2 \left|\frac{\partial\overline{u}}{\partial y}\right| \frac{\partial\overline{u}}{\partial y} \tag{2.6}$$

The distance l is called the Prandtl mixing length, for he was the first to use the above argumentation. It is a similar concept as the mean free path, used in molecular theories on viscosity.

In the vincinity of a solid boundary, the mixing length l is limited by the presence of the wall, and is therefore set proportional to the distance to the wall, according to $l = Ky$. The constant K is also known as the von Kármánn constant. This results in a Reynolds stress of

$$-\rho_0\overline{\tilde{u}\tilde{v}} = \rho_0 K^2 y^2 \left|\frac{\partial\overline{u}}{\partial y}\right| \frac{\partial\overline{u}}{\partial y} \tag{2.7}$$

2.2 Turbulent boundary layers due to a stationary mean flow

Now, returning to the problem for the stationary turbulent pipe flow with $\vec{\overline{v}} = (\overline{u}(y), 0, 0)$, the Navier-Stokes equation in the axial and radial direction for the turbulent flow reduces to

$$0 = -\frac{\partial \overline{p}}{\partial x} + \frac{\partial}{\partial y}\left(\eta \frac{\partial \overline{u}}{\partial y} - \rho_0 \overline{\tilde{u}\tilde{v}}\right) \tag{2.8}$$

$$0 = -\frac{\partial \overline{p}}{\partial y} - \frac{\partial \overline{\tilde{v}^2}}{\partial y} \tag{2.9}$$

in which the familiar boundary layer approximations have been made, with the y-coordinate defined as the distance to the wall.

This equation is valid for pipe flow as well as for a two-dimensional channel flow. In the following argumentation we will, for the sake of mathematical simplicity, derive the structure of the flow for the 2-D channel flow. It will turn out, that in the region of interest, very near the wall, the same relations hold for pipe flow [HIN 75].

Integration of the second equation with respect to y yields

$$\overline{p} + \rho \overline{\tilde{v}^2} \equiv p_{ext} \tag{2.10}$$

In this equation $\overline{\tilde{v}^2}$ is independent of x, so $\partial \overline{p}/\partial x = dp_{ext}/dx$. This is the external pressure gradient, acting as the driving force.

Integrating the first equation with respect to y yields

$$-y\frac{d\,\overline{p}_{ext}}{d\,x} + \eta \frac{\partial \overline{u}}{\partial y} - \rho_0 \overline{\tilde{u}\tilde{v}} + C = 0 \tag{2.11}$$

The integration constant C is determined by realising that at the wall the disturbance velocities must be zero, so that $-\rho_0 \overline{\tilde{u}\tilde{v}} = 0$, resulting in

$$C = -\eta \frac{\partial \overline{u}}{\partial y}\bigg|_{y=0} = -\tau_0 \tag{2.12}$$

τ_0 being the so-called wall shear stress. The other boundary condition, that in the middle of the channel the total shear stress must be zero, so

$$-\rho_0 \overline{\tilde{u}\tilde{v}} + \eta \frac{\partial \overline{u}}{\partial y}\bigg|_{y=h/2} = 0 \tag{2.13}$$

results in a relation between $d\overline{p}/dx$ and τ_0:

$$-\frac{h}{2}\frac{d\,p}{d\,x} = \tau_0 \tag{2.14}$$

completing the basic equation to one describing the velocity profile as function of the Reynold stress $\rho_0\overline{\tilde{u}\tilde{v}}$:

$$-\rho_0\overline{\tilde{u}\tilde{v}} + \eta\frac{\partial\overline{u}}{\partial y} = \tau_0 + y\frac{d\,\overline{p}}{d\,x} = \left(1 - \frac{2y}{h}\right)\tau_0 \tag{2.15}$$

Dividing this equation by τ_0, introducing the so-called friction velocity $u^{*2} = \tau_0/\rho_0$, as well as the previously found relation for the Reynold stress (2.7), results in:

$$\frac{K^2y^2}{u^{*2}}\left|\frac{\partial\overline{u}}{\partial y}\right|\frac{\partial\overline{u}}{\partial y} + \frac{\eta}{\rho_0 u^{*2}}\frac{\partial\overline{u}}{\partial y} = 1 - \frac{2y}{h} \approx 1 \tag{2.16}$$

$$\text{for: } y \ll h \tag{2.17}$$

Since the first term on the left varies with $y^2\left(\partial\overline{u}/\partial y\right)^2$, going to zero for $y \to 0$, whereas the other term varies only with $\partial\overline{u}/\partial y$, the region near the wall can be divided into two parts. One, very close to the wall, in which the viscous stresses dominate, and the other in which the turbulent Reynold stresses dominate. This division is even stricter than the above equation implies, since not only the mixing length $l = Ky$ tends to zero, but also the fluctuations $\tilde{v}$ and therefore $\tilde{u}$ vanish at the wall.

In order to estimate the thickness of the small laminar sublayer, the factor $\partial\overline{u}/\partial y$ is estimated by $C\partial\overline{u}/\partial y|_{y=0} = C\rho_0 u^{*2}/\eta$, since $\partial\overline{u}/\partial y$ will be of the same order as $\partial\overline{u}/\partial y|_{y=0}$ close to the wall. The critical value δ_l of y, determining the transition between the laminar sublayer and the turbulent layer then becomes $\delta_l = C\eta/K\rho_0 u^{*2}$. The velocity profile is then given by:

$$\frac{\overline{u}}{u^*} = \frac{\rho_0 u^*}{\eta}y \qquad \text{for: } 0 < y < \frac{C}{K}\frac{\eta}{\rho_0 u^*} = \delta_l \tag{2.18}$$

$$\frac{\overline{u}}{u^*} = \frac{1}{K}\ln y + C_2 \qquad \text{for: } y > \frac{C}{K}\frac{\eta}{\rho_0 u^*} = \delta_l \tag{2.19}$$

The integration constant C_2 can be determined by connecting the solutions in $y = C\eta/K\rho_0 u^{*2}$. This gives for the logarithmic layer the relation:

$$\frac{\overline{u}}{u^*} = \frac{1}{K}\left(\ln y + C - \ln\frac{C}{K}\frac{\eta}{\rho_0 u^*}\right) \tag{2.20}$$

$$= \frac{1}{K}\left(\ln\frac{\rho_0 u^*}{\eta}y + C - \ln\frac{C}{K}\right) \tag{2.21}$$

This last step is performed for two reasons. One is to seperate all the constants. These constants should be universal constants for the fully developped turbulent pipe flow, since the assumptions made in deriving this equation are all general assumptions. The second reason for separating is, that the equation is now dimensionless, giving the appropriate velocity and length scales as u^* resp. $\rho_0 u^*/\eta$. When making distances dimensionless with use of this scale factor, we denote them by a superscripted +, so

$$y^+ = y\frac{\rho_0 u^*}{\eta} \tag{2.22}$$

The constants can be determined by measurements on the profile of channel flow. These measurements are available from the literature and yield the relation [SCH 79]:

$$\frac{\overline{u}}{u^*} = 2.44\ln\frac{\rho_0 u^*}{\eta}y + 4.9 \tag{2.23}$$

from which follows that $K = 0.41$ and $C = 4.38$, so that the dimensionless thickness of the laminar sublayer $\delta_l^+ = C/K = 10.7$. The result for pipe flow usually is given as

$$\frac{\overline{u}}{u^*} = 2.5\ln\frac{\rho_0 u^*}{\eta}y + 5.5 \tag{2.24}$$

obtained from data measured by Nikuradse (see [HIN 75]) for smooth pipes, but these are the parameters fitted on the entire velocity distribution. Hinze [HIN 75] fitted the data obtained by Nikuradse again for the near-wall region, and obtained the same parameters as given for the 2-D channel flow.

It should be noted, that nothing has been said about the determination of the friction velocity u^*. It follows from a simple balance of forces on a piece of the pipe flow, that

$$u^{*2} = \frac{\tau_0}{\rho_0} = \frac{1}{\rho_0}\frac{\Delta p}{\Delta x}\frac{\mathcal{A}}{\mathcal{L}} \tag{2.25}$$

so it can be directly determined from measurement of $\Delta p/\Delta x$.

It can also be shown that the friction velocity u^* depends only on the Reynolds number. This relation of u^* on Re is given by the universal law of friction for smooth pipes,

$$\frac{1}{\sqrt{\psi}} = 2.0 \log Re\sqrt{\psi} - 0.8 \tag{2.26}$$

$$Re = \frac{\rho_0 U_0 2a}{\eta} \qquad \psi = 8\frac{u^{*2}}{U_0^2} \tag{2.27}$$

with ψ the dimensionless friction coefficient.

Now that the velocity profile is determined, the Reynold stress $\rho_0\overline{\tilde{u}\tilde{v}}$ can be determined as a function of $\overline{u}$ by (2.7). It is then possible to rewrite the Navier-Stokes equation in axial direction as follows:

$$0 = \frac{d\,\overline{p}}{d\,x} + \frac{\partial}{\partial y}\left[(\eta + \eta_t)\frac{\partial \overline{u}}{\partial y}\right] \tag{2.28}$$

with

$$\eta_t = 0 \qquad \text{for: } 0 < y < \delta_l^+ \frac{\eta}{\rho_0 u^*} = \delta_l \tag{2.29}$$

$$\eta_t = \rho_0 K^2 y^2 \left|\frac{\partial \overline{u}}{\partial y}\right| = K\rho_0 u^* y \qquad \text{for: } y > \delta_l^+ \frac{\eta}{\rho_0 u^*} = \delta_l \tag{2.30}$$

We see from this equation derived for an incompressible turbulent pipe flow, that the Navier-Stokes equation for the mean quantities keeps the same form as in the non-turbulent case, except for a change in the effective viscosity, due to the turbulent mixture. This extra apparent viscosity η_t is proportional to the distance to the wall, but vanishes completely in a small sublayer, which is therefore described by the equations for normal laminar flow. This sublayer is called the laminar sublayer. The turbulent layer is a logarithmic one, containing two undetermined constants, K and C/K, representing the relation between the transverse and longitudinal turbulent velocities, resp. the dimensionless thickness δ_l^+ of the laminar sublayer. The requirement for the two layers to meet at $y = \delta_l$, determines a relation between these constants.

Using this relation and measurements on the velocity profile of the turbulent logarithmic layer, the two constants can be determined, resulting in a

complete, semi-empirical theory of stationairy turbulent pipe flow. A picture of the resulting velocity profile is given figure 2.2.

It should be noted that in this treatment of turbulence, the transition between the laminar and turbulent zone is very sudden, this in contrast with to the more general treatment as found in [SCH 79], which assumes a buffer zone. This will turn out to be of major influence on the resulting attenuation.

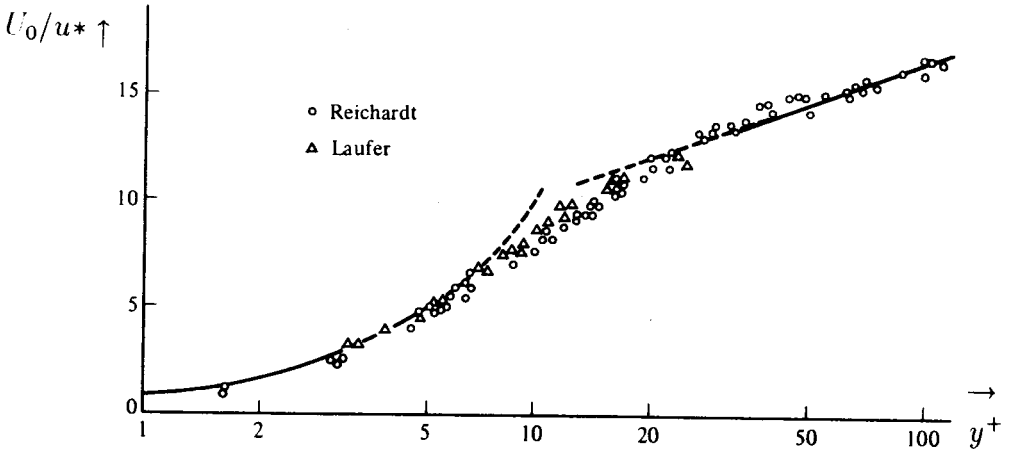

Figure 2.2: The dimensionless velocity $U_0/u*$ as function of y^+

2.3 Acoustical solution incorporating the effect of an axial mean flow.

The effect of a non-zero mean flow on the propagation of sound in the axial direction will be investigated. Variations of the mean flow in the axial direction will be neglected, *as well as the effects of viscosity and heat conduction in the bulk.* In the radial direction however, the mean velocity will vary from the maximum in the middle of the pipe, to zero at the wall, according to the fully developped turbulent pipe flow description derived in the previous section. So, when separating the physical quantities in a mean and a fluctuating part again, the velocity can be written as follows:

$$u = u_0(r) + u'(r,x) \quad u' \ll u_0 \ll c_0 \tag{2.31}$$

$$v_r = w_\phi = 0 \tag{2.32}$$

The linearized laws of conservation of mass, momentum and energy for the acoustical perturbations can be written in the form

$$\frac{\partial \rho}{\partial t} + u_0(r)\frac{\partial \rho}{\partial x} + \rho_0 \frac{\partial u}{\partial x} = \frac{D\,\rho}{D\,t} + \rho_0 \frac{\partial u}{\partial x} = 0 \tag{2.33}$$

$$\rho_0 \frac{\partial u}{\partial t} + \rho_0 u_0(r)\frac{\partial u}{\partial x} = \rho_0 \frac{D\,u}{D\,t} = -\frac{\partial p}{\partial x} \tag{2.34}$$

$$\rho_0 T_0 \frac{D\,s}{D\,t} = 0 \tag{2.35}$$

$$\text{with: } \frac{D}{D\,t} = \frac{\partial}{\partial t} + u_0(r)\frac{\partial}{\partial x}$$

in which the primes have been omitted again. Now, the recipy is used again to obtain a wave-equation for p. Therefore, ρ is eliminated by the thermodynamic relation (1.10). Then, in taking the total time derivative of (2.33), together with the axial derivative of (2.34), we get:

$$\frac{1}{c_0}\frac{D^2\,p}{D\,t^2} = \frac{\partial^2 p}{\partial x^2} \tag{2.36}$$

After averaging over the cross-section, we get:

$$\frac{1}{c_0^2}\left(U_0\frac{\partial}{\partial x} + \frac{\partial}{\partial t}\right)^2 p = \frac{\partial^2 p}{\partial x^2} \tag{2.37}$$

with U_0 the average of $u_0(r)$ over the cross-section of the pipe. This results in a dispersion relation for plane waves of the form $e^{\,i(k_m x - i\omega t)}$:

$$\left(ik_m M_0 - i\frac{\omega}{c_0}\right)^2 = (ik_m)^2 \tag{2.38}$$

$$k_{\pm m} = \pm\frac{\omega}{c_0}\frac{1}{1 \pm M_0} \tag{2.39}$$

$$\text{with: } M_0 = \frac{U_0}{c_0} \tag{2.40}$$

describing the propagation of sound incorporating the effect of a mean flow, M_0 representing the global Mach number, related to the mean velocity. Again, the other quantities are linearly related to p. The velocity u for example, can be deduced from equation (2.33), and is given by:

$$\hat{u}_\pm = \frac{\pm\hat{p}_\pm}{\rho_0 c_0}\left(\frac{1}{1 \pm [M_0 - m_0(r)]}\right) \tag{2.41}$$

with $m_0(r)$ the local Mach number $u_0(r)/c_0$. For the flow along the center line of the pipe this reduces approximately to the familiar relation

$$\hat{u}_\pm = \frac{\pm\hat{p}_\pm}{\rho_0 c_0} \tag{2.42}$$

whereas for the region near the wall, the relation becomes

$$\hat{u}_\pm = \frac{\pm k_{\pm m}\hat{p}_\pm}{\rho_0 \omega} \tag{2.43}$$

The temperature T still obeys the simpler relation

$$\hat{T}_\pm = \frac{T_0\beta}{\rho_0 c_p}\hat{p}_\pm \tag{2.44}$$

2.4 acoustical boundary layer in case of a turbulent mean flow

In the previous section, a dispersion relation describing the propagation of sound in a pipe with flow, neglecting the effects of viscosity and heat conduction, has been derived. It will serve as a basis to examine the structure of the acoustical boundary layer, which is the main cause of attenuation of sound in a pipe. Considering the attenuation as a small effect, we can use the approximate dispersion relation found to estimate the spacial derivatives. We will use the time-averaged Navier-Stokes equation (2.4) in the boundary layer approximation, and write the physical quantities Q, conform equation (2.1), as

$$Q = \overline{Q} + \tilde{Q} = Q_0 + Q' + \tilde{Q}_0 + \tilde{Q}' \tag{2.45}$$

which is equivalent with stating that *the acoustical variations can be regarded quasistationary with respect to the turbulent variations.* An other way of saying this, is that the acoustical variations take place on a time scale much larger than the fluctuating turbulent motions. The averaging time is then choosen so long that the turbulent fluctuations are averaged out, but short enough to allow an oscillating acoustical variation of the mean quantity to exist. The result is:

$$\rho_0 \frac{\partial u'}{\partial t} - \rho_0 u_0(y) \frac{\partial u'}{\partial x} = -\frac{\partial p_0}{\partial x} - \frac{\partial p'}{\partial x} + \frac{\partial}{\partial y}\left[\eta\left(\frac{\partial u_0}{\partial y} + \frac{\partial u'}{\partial y}\right) - \rho_0 \overline{\tilde{u}\tilde{v}}\right] \tag{2.46}$$

The Reynold stress was estimated by (2.7):

$$-\rho_0 \overline{\tilde{u}\tilde{v}} = \rho_0 K^2 y^2 \left|\frac{\partial u_0}{\partial y} + \frac{\partial u'}{\partial y}\right| \left(\frac{\partial u_0}{\partial y} + \frac{\partial u'}{\partial y}\right) \tag{2.47}$$

If $\partial u'/\partial y < \partial u_0/\partial y$, we get after performing the multiplication, using equation (2.30):

$$-\rho_0 \overline{\tilde{u}\tilde{v}} = \eta_t \left(\frac{\partial u_0}{\partial y} + 2\frac{\partial u'}{\partial y}\right) + \rho_0 K^2 y^2 \left(\frac{\partial u'}{\partial y}\right) \left|\frac{\partial u'}{\partial y}\right| \tag{2.48}$$

where η_t is defined on basis of the stationary flow velocity u_0. Inserting this in the above Navier-Stokes equation leads to an equation, equivalent to

that describing the stationary equation for turbulent pipe flow, except for the terms involving the small acoustical perturbations. We see that, if there are no acoustical disturbances, the equation is exactly the stationary one, for which we know the solution. So the stationary equation (2.28) can be substracted to obtain an equation for the acoustical quantities. In doing so, and neglecting the term $(\partial u'/\partial y)|\partial u'/\partial y|$, the result is:

$$\rho_0 \frac{\partial u'}{\partial t} - \rho_0 u_0(r) \frac{\partial u'}{\partial x} = -\frac{\partial p'}{\partial x} + \frac{\partial}{\partial y}\left[(\eta + 2\eta_t)\frac{\partial u'}{\partial y}\right] \tag{2.49}$$

in which u_0 is given by the solution of the stationary equation. This equation must be solved under the condition that $u'(0) = 0$. The other boundary condition, for $y \to \infty$, will be governed by the thickness of the acoustical boundary layer δ_v in comparison to the turbulent boundary layer thickness δ_t. When taking the limit for $\omega \to \infty$, so that $\delta_v \ll \delta_t$, the second term on the left will be negligible, since the acoustical shear wave will be damped completely before entering the area in which u_0 is significantly greater then zero. The resulting error will be of order $O(m_0(\delta_v))$. The boundary condition then becomes, in complex notation, omitting the primes:

$$\hat{u}(\infty) = \frac{k_m}{\rho_0 \omega}\hat{p} \tag{2.50}$$

in which k_m is the wavenumber for the acoustical solution with mean flow as given in (2.39). Using the following relation for the apparent viscosity η_t:

$$\eta_t(y) = 0 \qquad \text{for: } 0 < y < \delta_l \tag{2.51}$$

$$\eta_t(y) = \rho_0 K u^*(y - y_0) \qquad \text{for: } y > \delta_l \tag{2.52}$$

the solution to (2.56) can be given in terms of Hankelfunctions. It must be noted that this relation is slightly different from that derived in section 2.2, with respect to the factor y_0. This factor y_0 is an arbitrary constant. We will use this relation, since it is a more general description of the apparent viscosity.

The particular solution to the problem

$$\hat{u}_p = \frac{k_m \hat{p}}{\rho_0 \omega} \tag{2.53}$$

is substracted from the equation, altering the boundary conditions to:

$$u(0) = -\frac{k\hat{p}}{\rho_0\omega} \tag{2.54}$$

$$u(\infty) = 0 \tag{2.55}$$

and leaving to be solved:

$$\rho_0\frac{\partial u'}{\partial t} = \frac{\partial}{\partial y}\left[(\eta + 2\eta_t)\frac{\partial u'}{\partial y}\right] \tag{2.56}$$

For $y < \delta_l$, the problem is similar to that of the viscous boundary layer in the absence of mean flow, so the solution is of the form:

$$\hat{u}_1 = A_1 e^{-\epsilon_v y} + A_2 e^{\epsilon_v y} \tag{2.57}$$

$$\text{with: } \epsilon_v = \sqrt{\frac{-i\omega\rho_0}{\eta}} \tag{2.58}$$

Satisfying the boundary condition for $y = 0$, results in:

$$\hat{u}_1 = A_2\left(e^{\epsilon_v y} - e^{-\epsilon_v y}\right) - \frac{k_m\hat{p}}{\rho_0\omega}e^{-\epsilon_v y} = \frac{k\hat{p}}{\rho_0\omega}\left(A\sin(i\epsilon_v y) - e^{-\epsilon_v y}\right) \tag{2.59}$$

The reason for the decomposition of A_2 in $Ak_m\hat{p}/\rho_0\omega$ is that it simplifies the final expressions. The solution to the equation for $y > \delta_l$ can be found in terms of Bessel-functions, since the equation can be rewritten to take the form of Bessels equation:

$$x\frac{\partial}{\partial x}\left(x\frac{\partial y}{\partial x}\right) + (x^2 - \nu^2)y = 0 \tag{2.60}$$

with ν a constant. Writing (2.56) somewhat differently, we get the following homogeneous differential equation:

$$\frac{\partial}{\partial y}\left[\left(\frac{\eta}{2Ku^*\rho_0} + y - y_0\right)\frac{\partial\hat{u}}{\partial y}\right] + \frac{i\omega}{2Ku^*}\hat{u} = 0 \tag{2.61}$$

Now, when making the substitution

$$\xi = \sqrt{\frac{\eta}{2Ku^*\rho_0} + y - y_0} \tag{2.62}$$

$$\partial y = 2\xi\partial\xi \tag{2.63}$$

the equation becomes:

$$\frac{\partial}{\partial\xi}\left(\xi\frac{\partial\hat{u}}{\partial\xi}\right)+\frac{2i\omega}{Ku^*}\xi\hat{u}=0 \tag{2.64}$$

The first term now has the required form, but the second term contains the unwanted factor $2i\omega/Ku^*$. In writing

$$\zeta = \sqrt{\frac{2i\omega}{Ku^*}}\xi \tag{2.65}$$

$$\partial\zeta = \sqrt{\frac{2i\omega}{Ku^*}}\partial\xi \tag{2.66}$$

we obtain

$$\frac{\partial}{\partial\zeta}\left(\zeta\frac{\partial\hat{u}}{\partial\zeta}\right)+\zeta\hat{u}=0 \tag{2.67}$$

This is a Bessel equation with $\nu = 0$, so the solution is a linear combination of Bessel-functions of order zero. In order to obey the boundary condition for $y \to \infty$, being $\hat{u} \to 0$, the solution must be a Hankel-function. Since $\zeta \sim (1+i)\sqrt{y}$, y real, the solution is the first Hankel-function of order zero. So, for $y > \delta_l$,

$$\hat{u}_2 = B_1 H_0^1(\zeta) = \frac{k\hat{p}}{\rho_0\omega}BH_0^1(\zeta) \tag{2.68}$$

$$\zeta = \sqrt{\frac{2i\omega}{Ku^*}}\xi = a\sqrt{1+\frac{2\eta_t(y)}{\eta}} \tag{2.69}$$

$$\text{with: } a = \frac{i\eta\epsilon_v}{Ku^*\rho_0} = \frac{1+i}{K\delta_v^+} \tag{2.70}$$

The solutions $\hat{u}_1$ and $\hat{u}_2$ must now be matched at $y = \delta_l$. In doing so, both the velocity $\hat{u}$ and the shear stress $\eta\partial\hat{u}/\partial y$ must be matched at $y = \delta_l$. The following property of Hankel-functions is used to calculate the first derivative of $\hat{u}_2$.

$$H_n(\zeta) = (-2\zeta)^n\frac{\partial^n H_0(\zeta)}{\partial(\zeta^2)^n} \tag{2.71}$$

Because $\partial\zeta^2 = (2i\omega/Ku^*)\partial y$, the result is:

$$\frac{\partial \hat{u}_2}{\partial y} = B\frac{2i\omega}{Ku^*}\frac{\partial H_0^1(\zeta)}{\partial \zeta^2} = B\frac{2i\omega}{Ku^*}\frac{1}{-2\zeta}H_1^1(\zeta) \tag{2.72}$$

So by requiring $\hat{u}_1(\delta_l) = \hat{u}_2(\delta_l)$ and $\eta\hat{u}_1'(\delta_l) = (\eta + 2\eta_t(\delta_l))\hat{u}_2'(\delta_l)$, a closed set of equations for A and B is obtained

$$BH_0^1(ac) = A\sin b - e^{\,ib} \tag{2.73}$$

$$c^2 B\frac{-i\omega}{Ku^*ac}H_1^1(ac) = B\frac{-i\epsilon_v}{c}H_1^1(ac) = Ai\epsilon_v\cos b + \epsilon_v e^{\,ib} \tag{2.74}$$

$$\text{with: } b = i\delta_l\epsilon_v = \frac{(1+i)\delta_l^+}{\delta_v^+} \tag{2.75}$$

$$c = \sqrt{1 + \frac{2\eta_t(\delta_l)}{\eta}} = \sqrt{1 + 2K(\delta_l^+ - y_0^+)} \tag{2.76}$$

So the solutions are:

$$A = \frac{[cH_1^1(ac) + iH_0^1(ac)]\,e^{\,ib}}{H_0^1(ac)\cos b + cH_1^1(ac)\sin b} \tag{2.77}$$

$$B = \frac{-1}{H_0^1(ac)\cos b + cH_1^1(ac)\sin b} \tag{2.78}$$

The total solution is therefore given by:

$$\begin{aligned}\hat{u} &= \frac{k_m\hat{p}}{\rho_0\omega}\left[\frac{(cH_1^1(ac) + iH_0^1(ac))\sin(i\epsilon_v y)e^{\,ib}}{H_0^1(ac)\cos b + cH_1^1(ac)\sin b} + \left(1 - e^{\,-\epsilon_v y}\right)\right] \\ &\quad \text{for: } 0 \le y < \delta_l \\ &= \frac{k_m\hat{p}}{\rho_0\omega}\left[1 - \frac{H_0^1\left(a\sqrt{1 + \frac{2\eta_t(y)}{\eta}}\right)}{H_0^1(ac)\cos b + cH_1^1(ac)\sin b}\right] \\ &\quad \text{for: } y \ge \delta_l\end{aligned} \tag{2.79}$$

With the constants a, b and c defined as:

$$a = \frac{1+i}{K\delta_v^+};\quad b = \frac{(1+i)\delta_l^+}{\delta_v^+};\quad c = \sqrt{1 + 2K(\delta_l^+ - y_0^+)} \tag{2.80}$$

With this explicit expression for the velocity in the boundary layer an estimate can be made on the attenuation as a result of the viscosity $\eta + 2\eta_t$.

Some special and limiting cases of the used model for the turbulent viscosity can be calculated.

When increasing the turbulent intensity to ∞ for $y > \delta_l$ by enlarging K , we arive at the so-called rigid-plate model, as proposed by Ronneberger [RON 77], in which the acoustical shear wave is completely reflected at the boundary between the laminar and logarithmic layer. It can be derived directly by setting $u(y > \delta_l) = u_{ac}$ and matching the solution for $y < \delta_l$ to this boundary condition.

If the effect of turbulence is neglected, by setting the $K = 0$, or the laminar boundary layer thickness δ_l^+ to ∞, the Kirchhoff solution is found, because then A becomes zero.

If the boundary layer thickness δ_l^+ is set to zero, as well as y_0^+, the solution found in the first paper of Howe turns up [HOW 79].

In the special case that $y_0^+ = \delta_l^+$, the solution given by Howe in a second paper [HOW 84] is the result, since then $c = 1$.

When setting $y_0 = 0$, the turbulent viscosity takes the form derived in section 2.2. This model will be referred to as the new model or the new theory, since it is an adaptation of the existing model used by Howe.

An expression for the thermo-acoustical boundary layer has yet to be determined. Therefore the linearized energy equation in case of a mean flow is used:

$$\rho_0 T_0 \frac{\partial s'}{\partial t} + \rho_0 T_0 u_0(r) \frac{\partial s'}{\partial x} = \frac{\partial}{\partial y}\left[(\kappa + 2\kappa_t)\frac{\partial T'}{\partial y}\right] \tag{2.81}$$

The thermal conduction is assumed to behave in a similar way as the viscosity, the two being related by

$$\kappa_t = \frac{\eta_t c_p}{Pr_t} \tag{2.82}$$

with Pr_t the turbulent Prandtl number. Measurements on Pr_t have been performed, resulting in a value of $0.7 < Pr_t < 0.9$ [SCH 79]. The energy equation then is rewritten, using the thermodynamic relation (1.6), resulting in an equation equivalent with that for the boundary layer velocity:

$$\rho_0 c_p \left[\frac{\partial (T' - T'_{ac})}{\partial t} + u_0(r)\frac{\partial (T' - T'_{ac})}{\partial x}\right] = \frac{\partial}{\partial y}\left[(\kappa + 2\kappa_t)\frac{\partial T'}{\partial y}\right] \tag{2.83}$$

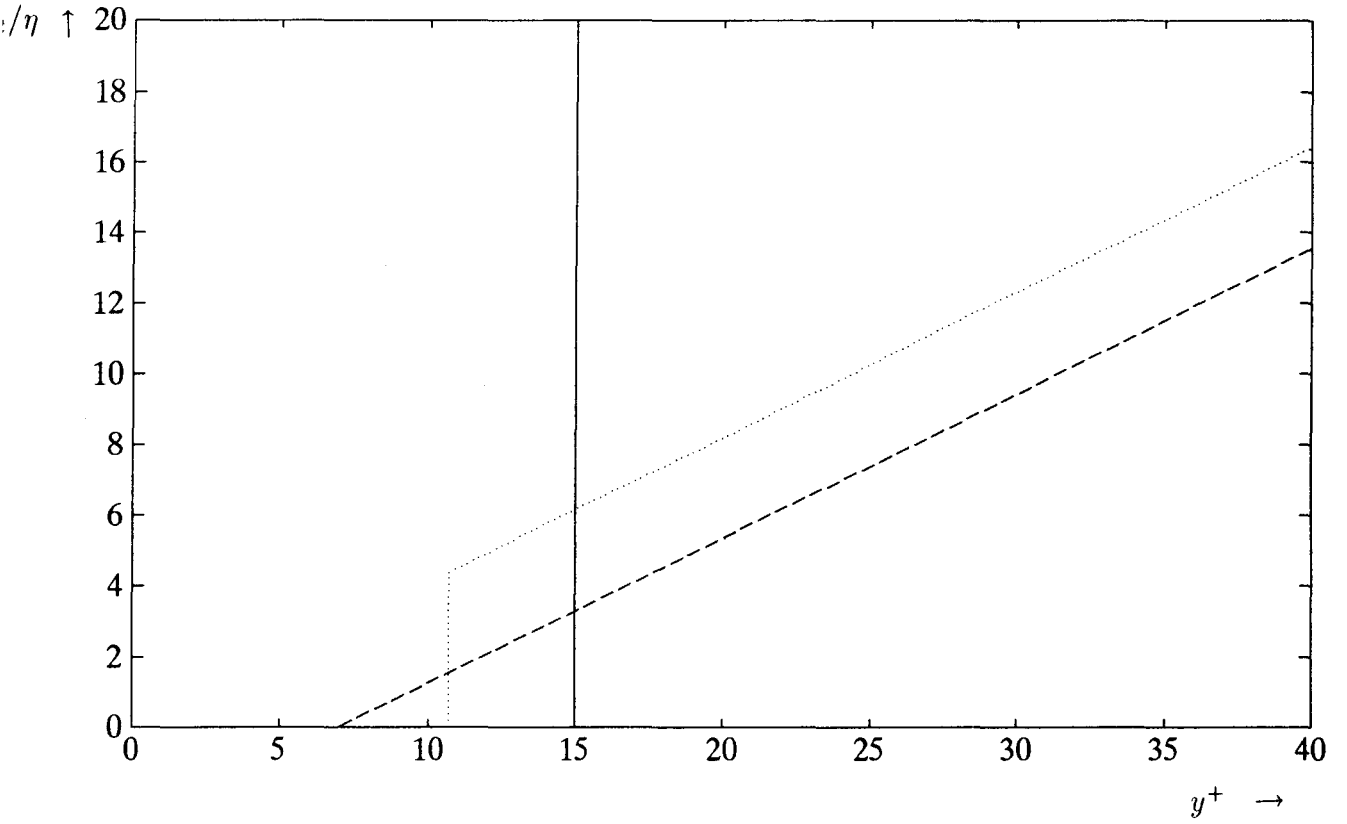

Figure 2.3: The different models for η_t.
η_t/η as function of y^+.
—— rigid plate; - - - Howe ($y_0^+ = \delta_l^+$); · · · new model ($y_0^+ = 0$)

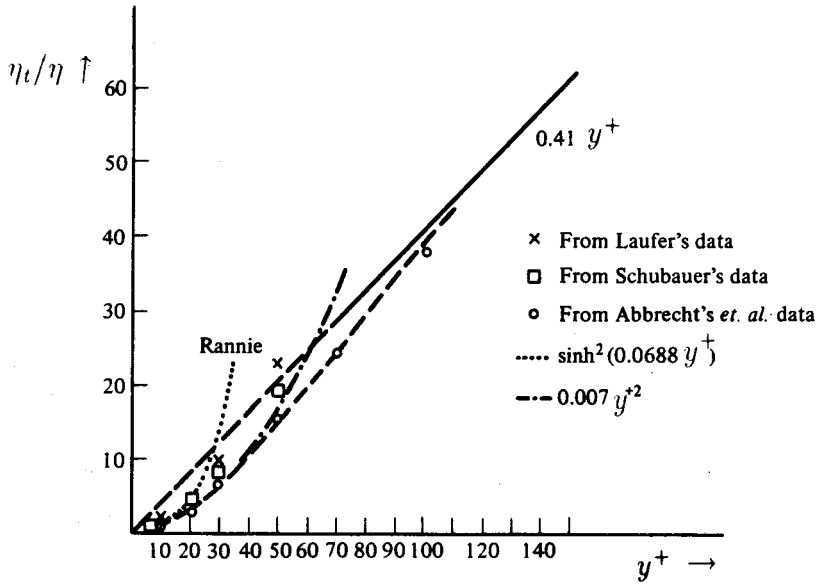

Distribution of eddy viscosity near the wall in pipe flow. (Adapted from: *Laufer J.*;[41] *Abbrecht, P. H., and S. W. Churchill*[52]), and in boundary-layer flow. (Adapted from: *Schubauer, G. B.*[30])

Figure 2.4: Measurement of η_t/η as function of y^+.

The solution to this equation, under the same assumptions as above, can be found by making the obvious substitutions in (2.79).

$$T = T_{ac}\left(A' \sin(i\epsilon_T y) - e^{-\epsilon_T y}\right) \tag{2.84}$$

$$= \frac{T_0\beta}{\rho_0 c_p} p \left(A' \sin(i\sqrt{Pr}\epsilon_v y) - e^{-\sqrt{Pr}\epsilon_v y}\right) \tag{2.85}$$

$$\text{with: } A' = A(a', b', c') \tag{2.86}$$

$$a' = \frac{Pr_t}{\sqrt{Pr}} a; \quad b' = b\sqrt{Pr}; \quad c' = \sqrt{1 + \frac{Pr}{Pr_t} 2K(\delta_l^+ - y_0^+)} \tag{2.87}$$

This enables us to incorporate the effect of turbulent heat transport in the calculation of the attenuation due to the boundary layers. A calculation of this kind was first performed by Howe [HOW 84].

2.5 Viscothermal attenuation of plane waves due to boundary layers in case of a turbulent mean flow.

In having an expression for the acoustical boundary layers in case of an turbulent mean flow, we're able to calculate the attenuation due to these boundary layers in a way similar to that of section (1.5). Again, the equations of mass and momentum conservation are used, neglecting the effects of viscosity and heat conduction, except for the region close to the wall, where the boundary layer solutions are used. This means that the attenuation in the bulk of the fluid due to viscosity and heat conduction, molecular as well as turbulent, is neglected. That the turbulent bulk attenuation can be neglected in comparison to the attenuation due to the boundary layers, has been shown by Howe [HOW 79]. So we write:

$$\frac{D\,\rho}{D\,t} + \rho_0 \frac{\partial u}{\partial x} = 0 \tag{2.88}$$

$$\rho_0 \frac{D\,u}{D\,t} = -\frac{\partial p}{\partial x} + \frac{\partial}{\partial y}\left[(\eta + 2\eta_t)\frac{\partial u}{\partial y}\right] \tag{2.89}$$

completed with the energy equation and the equation relating ρ, p and s

$$\rho_0 T_0 \frac{D\,s}{D\,t} = \frac{\partial}{\partial y}\left[(\kappa + 2\kappa_t)\frac{\partial T}{\partial y}\right] \tag{2.90}$$

$$\rho = \frac{1}{c_0^2} p - \frac{\rho_0 \beta T_0}{c_p} s \tag{2.91}$$

and after taking the total time derivative of (2.88) and taking the axial derivative of (2.89), substracting them, and eliminating ρ with help of (2.90) and (2.91), we get:

$$\frac{1}{c_0^2}\frac{D^2\,p}{D\,t^2} - \frac{\beta}{c_p}\frac{D}{D\,t}\frac{\partial}{\partial y}\left[(\kappa + 2\kappa_t)\frac{\partial T_{bl}}{\partial y}\right] \tag{2.92}$$

$$= \frac{\partial^2 p}{\partial x^2} - \frac{\partial}{\partial x}\frac{\partial}{\partial y}\left[(\eta + 2\eta_t)\frac{\partial u_{bl}}{\partial y}\right] \tag{2.93}$$

Performing the integration over the cross-section as in section 1.5 results in

$$\left[\frac{1}{c_0^2}\left(\frac{\partial}{\partial t}+U_0\frac{\partial}{\partial x}\right)^2-\frac{\partial^2}{\partial x^2}\right]p= \tag{2.94}$$

$$\frac{\mathcal{L}}{\mathcal{A}}\left[(\eta+2\eta_t)\frac{\partial}{\partial x}\left.\frac{\partial u_{bl}}{\partial y}\right|_{y=0}-\frac{\beta(\kappa+2\kappa_t)}{c_p}\frac{\partial}{\partial t}\left.\frac{\partial T_{bl}}{\partial y}\right|_{y=0}\right] \tag{2.95}$$

in which the factor $u_0\partial T_{bl}/\partial x$ has been neglected in calculating the integral with respect to $\partial T_{bl}/\partial t$, since near the wall $u_0 k \ll \omega$. When again assuming plane harmonic waves, and renaming the righthand side expression divided by p as $F(k,\omega)$, we get the following dispersion relation:

$$\left(ikM-i\frac{\omega}{c_0}\right)^2+k^2=F(k,\omega) \tag{2.96}$$

Since the attenuation is assumed to change the free-space wave number k_m only slightly, the function F can estimated by setting $F=F(k_m,\omega)$, because it contains only product terms of k with small quantities. The dispersion relation can than be re-expressed as follows:

$$(1-M^2)k^2+\frac{2M\omega}{c_0}k-\left(\frac{\omega^2}{c_0^2}+F(k_m,\omega)\right)=0 \tag{2.97}$$

resulting in

$$k_\pm = \frac{-\frac{2M\omega}{c_0}\pm\sqrt{\frac{4M^2\omega^2}{c_0^2}+4(1-M^2)\left(\frac{\omega^2}{c_0^2}+F(k_{\pm m},\omega)\right)}}{2(1-M^2)} \tag{2.98}$$

$$= \frac{-\frac{M\omega}{c_0}\pm\sqrt{\frac{\omega^2}{c_0^2}+(1-M^2)F(k_{\pm m},\omega)}}{1-M^2} \tag{2.99}$$

$$\approx \frac{-\frac{M\omega}{c_0}\pm\left[\frac{\omega}{c_0}+\frac{(1-M^2)c_0}{2\omega}F(k_{\pm m},\omega)\right]}{1-M^2} \tag{2.100}$$

$$= \pm\frac{\omega}{c_0}\frac{1}{1\pm M}\pm\frac{c_0}{2\omega}F(k_{\pm m},\omega) \tag{2.101}$$

The attenuation thus can be expressed as:

$$\alpha_\pm=\pm\frac{c_0}{2\omega}F(k_{\pm m},\omega) \tag{2.102}$$

Evaluation of F by using the solution of the boundary layer equations (2.79) results in the following expression for the attenuation:

$$\alpha_{\pm} = \pm \left(\frac{1 + iA}{(1+M)^2} + \frac{(\gamma - 1)(1 + iA')}{\sqrt{Pr}} \right) (1 + i)\alpha_v \tag{2.103}$$

with A and A' conform equations (2.77) and (2.86), as found in the previous section, and α_v the real part of the attenuation as it would be only resulting from a zero mean flow viscous boundary layer, as in equation (1.55).

It must be noted that this attenuation is a complex quantity. The imaginary part determines the amplitude decay along the pipe, whereas the real part introduces a change in the fase velocity of the sound wave.

Some comment must be given on the method used to come to this attenuation. The acoustical boundary layer description is derived under the assumption that the acoustical shear wave stays completely within the turbulent boundary layer, resulting in the boundary condition $\hat{u}(\infty) = k\hat{p}/\rho_0\omega$. This assumption is fullfilled for a fixed small Mach number in the limit that $\omega \to \infty$.

On the other hand, if for fixed ω the Mach number is taken to zero, so that the shear wave is completely in the turbulent region, the boundary condition should be altered to $\hat{u}(\infty) = \hat{p}/\rho_0 c_0$. But in this limit of $M \to 0$, $k \approx \omega/c_0$, so the expression for the attenuation remains valid.

Therefore it is argued that the above expression for the attenuation is an apropriate one for the intermediate combinations of M and ω.

2.5.1 Implications for measurement

When making measurements, we want to seperate the Mach number dependence from that on the dimensionless viscous length scale δ_v^+. Also, we want to normalize the measurement in some way. Therefore, we will plot the attenuation as found above, however without any Mach dependence, normalized by the Kirchhoff*amplitude*attenuation $i\Im(\alpha_0)$. We're mainly interested in the*imaginary part of the attenuation*, since that causes the amplitude attenuation, which has now become the*real part of the normalized attenuation.* So, we will plot

$$\lim_{M \to 0}^{\delta_l^+ fixed} \frac{\alpha_{\pm}}{i\alpha_0} = \frac{1+i}{i} \frac{1 + iA + \frac{\gamma-1}{\sqrt{Pr}}(1 + iA')}{1 + \frac{\gamma-1}{\sqrt{Pr}}} \equiv \frac{Z_\tau + \frac{\gamma-1}{\sqrt{Pr}} Z_q}{1 + \frac{\gamma-1}{\sqrt{Pr}}} = Z_{tot} \tag{2.104}$$

We've introduced the dimensionless functions Z_τ and Z_q, known as the dimensionless wall impedances of the sound wave. They are defined as the wall impedances,

$$z_\tau = \left.\frac{\hat{\tau}}{\hat{u}_{ac}}\right|_{y=0} \tag{2.105}$$

$$z_q = \left.\frac{\hat{\Phi}}{\hat{T}_{ac}}\right|_{y=0} \tag{2.106}$$

$$\text{with: } \hat{\tau} = -\eta\frac{\partial \hat{u}_{ac}}{\partial y};\quad \hat{\Phi} = -\kappa\frac{\partial \hat{T}_{ac}}{\partial y} \tag{2.107}$$

made dimensionless by the value resulting for the Kirchhof estimate:

$$Z_\tau = z_\tau\frac{\delta_v}{\eta} \tag{2.108}$$

$$Z_q = z_q\frac{\delta_T}{\kappa} = z_q\frac{\delta_v}{\kappa\sqrt{Pr}} \tag{2.109}$$

These impedancies Z_τ, Z_q and Z_{tot} will be used in this report only as abbreviation, and there will be no inquiry on the physical background of the similarity between the theoretical results obtained here for the attenuation and the results obtained by others on basis of the impedance. We have plotted the total impedance for the different models for the effective viscosity in figure 2.5, using $Pr_t = Pr$. When we look at the real part, we see a low region limit of unity, a typical dip for $\delta_v^+ \approx \delta_l^+$, and a straight line with a certain slope, looking identical for the three models. The low region limit shows that the attenuation attains the form of the Kirchhoff attenuation. The dip is thought to be a result of interference of the shear wave with it's reflection at the edge of the turbulent zone. The slope will turn out to be of importance in determining the static limit, since it is proportional to the attenuation for low frequencies. Therefore, we take a closer look at the slope for the different models.

We want to determine the behaviour of Z_τ for large δ_v^+. When we look at the rigid plate model, as introduced in section 2.4, A takes the following form:

$$A = \frac{e^{\,ib}}{\sin b} \tag{2.110}$$

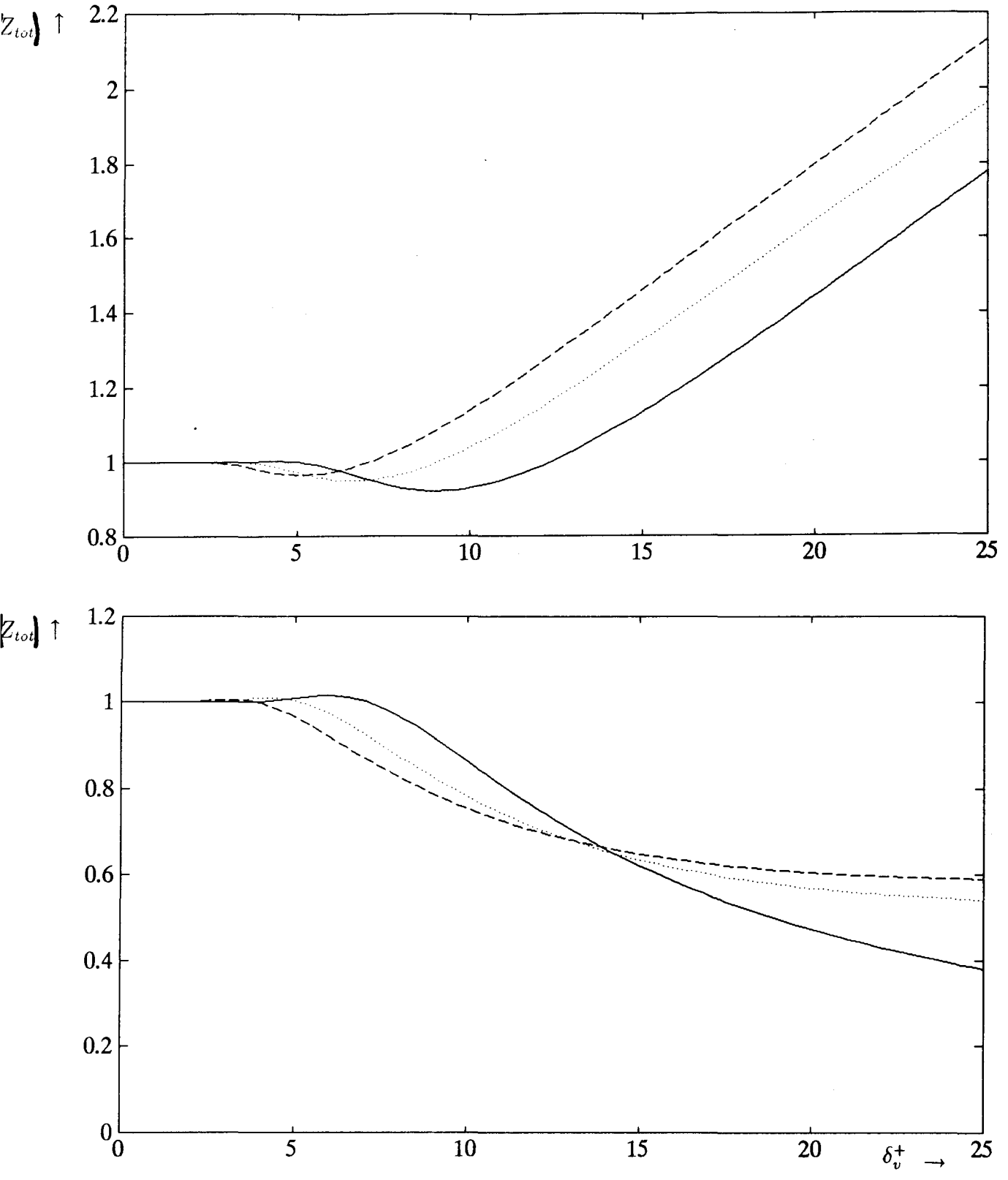

Figure 2.5: Theoretical form of $\Re\{Z_{tot}\}$(above) and $\Im\{Z_{tot}\}$(below) as function of δ_v^+
— rigid plate limit ($\delta_l^+ = 15$)
- - Howe ($y_0^+ = \delta_l^+ = 7$)
· · · new model($y_0^+ = 0$; $\delta_l^+ = 10.7$)

$$\text{with: } b = \frac{(1+i)\delta_l^+}{\delta_v^+} \tag{2.111}$$

If we expand it into power series for large δ_v^+, so for small b, we get the following result:

$$A = \frac{1+ib}{b} = 1/b \tag{2.112}$$

$$= \frac{(1-i)\delta_v^+}{2\delta_l^+} \tag{2.113}$$

So, we get:

$$\lim_{\delta_v^+ \to \infty} 1 + iA = \frac{i(1-i)\delta_v^+}{2\delta_l^+} \tag{2.114}$$

Returning to Z_τ, we get:

$$\lim_{\delta_v^+ \to \infty} Z_\tau = \frac{1+i}{i}(1+iA) = \frac{\delta_v^+}{\delta_l^+} \tag{2.115}$$

We see that the slope tends to a limiting value of $1/\delta_l^+$. For the other two models, we just state that the slope will go to zero for $\delta_v^+ \to \infty$. This will occur however for values of δ_v^+ far beyond the valid range, determined by the dimensions of the pipe in relation to the thickness δ_v. In the region of interest, for $\delta_v^+ \approx 30$, the slope will vary only slowly, as can be seen in figure 2.5.

Chapter 3

Some other theories from literature

3.1 The stationary limit

We can imagine that for very low frequencies, the attenuation of sound could be determined by the same mechanisms as those responsible for the static pressure drop in fully developped turbulent pipe flow. Therefore, we could expand the static pressure drop in a taylor series, from which we will only use the first term. That is to say, we linearize the behaviour of the pressure drop due to a small periodical change in the mean velocity. For the static pressure drop we write:

$$\frac{d\,p_0}{d\,x} = \frac{\psi}{2a}\frac{\rho_0}{2}U_0^2 \tag{3.1}$$

in which ψ is the dimensionless friction factor. Variation of U_0 by introducing a disturbance u', results in change in the pressure drop p':

$$\frac{d\,p_0 + p'}{d\,x} = \frac{\psi}{2a}\frac{\rho_0}{2}(U_0 + u')^2 = \frac{\psi}{2a}\frac{\rho_0}{2}(U_0^2 + 2U_0u' + u'^2) \tag{3.2}$$

$$\frac{d\,p'}{d\,x} = \frac{\psi}{2a}\rho_0 U_0 u' \tag{3.3}$$

If we now assume the relation $p' = \rho_0 c_0 u'$ for plane waves is still valid, we come to the expression:

$$\frac{d\,p'}{d\,x} = \frac{\psi}{2a}\frac{U_0}{c_0}p' = \frac{\psi}{2a}M_0 p' \tag{3.4}$$

Since the attenuation α is described by $p'(x) = p'(0)e^{-\alpha x}$, we see that:

$$\alpha_{stat} = \frac{\frac{d\,p'}{d\,x}}{p'} = \frac{\psi M}{2a} \tag{3.5}$$

This is the attenuation due to a uniform pressure drop. Since we're considering harmonic oscillations, we must take the effective average over one period, resulting in halve the value found above. So,

$$\alpha_{stat} = \frac{i\psi M}{4a} \tag{3.6}$$

the additional i is introduced because we actually determined the imaginairy part of the attenuation as defined in equation (1.25). When making dimensionless again with $i\alpha_0$, we get the following equation for Z_{tot}:

$$Z_{tot} = \frac{\psi M}{4a\alpha_0} = \frac{\delta_v +}{1 + \frac{\gamma - 1}{\sqrt{Pr}}} \sqrt{\frac{\psi}{2}} \tag{3.7}$$

A more detailed description of the theory of this static limit is given by Ingard and Singhal [ING 74].

3.2 The quasi-laminar limit

As we've found in the previous chapter, when $\delta_v \ll \delta_l$ the attenuation can actually be described by the Kirchhoff attenuation, altered for the up- and downstream direction of propagation according to the Doppler effect. This shift is essentially caused for two reasons. One is that the wavenumber is affected by the mean flow, so:

$$k_{\pm m} = \frac{\omega}{c_0} \frac{1}{1 \pm M} \tag{3.8}$$

The other reason is that the equations governing the shear waves contain convective terms involving the mean velocity profile, such as $u_0 \partial/\partial x$. In our approach we simply neglected the convective terms in the wall region, by assuming that this will cause only a minor error.

Ronneberger [RON 77] has made a very thourough investigation on the effects of these terms, and has also included the influence of the pressure gradients along the pipe due to the friction and the pressure gradients in the axial direction due to turbulent dissipation. He performed his calculations for the attenuation of sound using only the molecular viscosity η, so neglecting the turbulent viscosity η_t.

His theory describes how a sound wave should propagate theoretically, under the influence of a mean velocity profile, in our case of course the turbulent profile. It does not include any interaction of the turbulence with the acoustical field.

The result of his investigation is a relation for the attenuation, in which the difference in up- and downstream attenuation is described by three dimensionless functions. These functions depend only on the Mach number, and have been calculated for air.

$$\alpha = \alpha_v \sqrt{\frac{1}{P_w}} (\zeta_0 - \zeta_1^* \epsilon^* - \zeta_1 \epsilon) \tag{3.9}$$

$$\text{with: } P_w = 1 - 0.18M^2, \quad \epsilon = -\frac{(1+i)\eta}{2\rho_0 c_0} \delta_v \tag{3.10}$$

In the figure 3.1, the ratio ϵ^*/ϵ is plotted as function of δ_v^+. In the following three figures 3.2 , 3.4 and 3.3, the dimensionless functions are plotted against the Mach number.

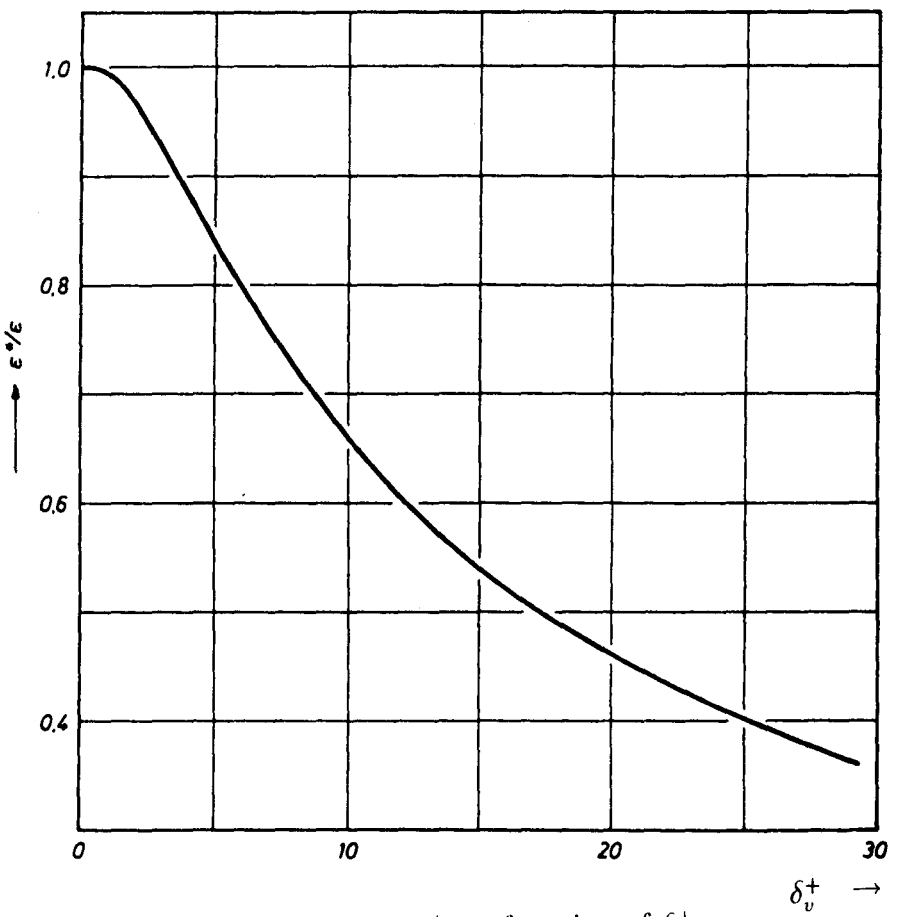

Figure 3.1: ϵ^*/ϵ as function of δ_v^+

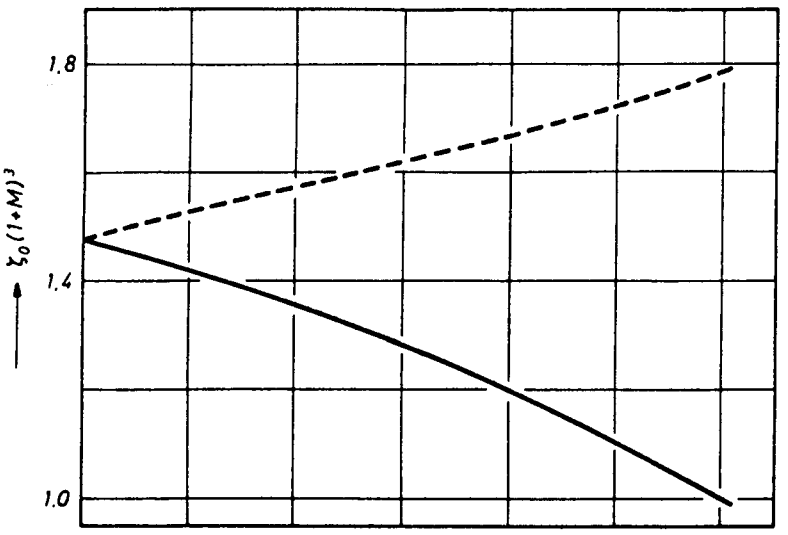

Figure 3.2: $\zeta_0(1 + M)^3$ as function of M

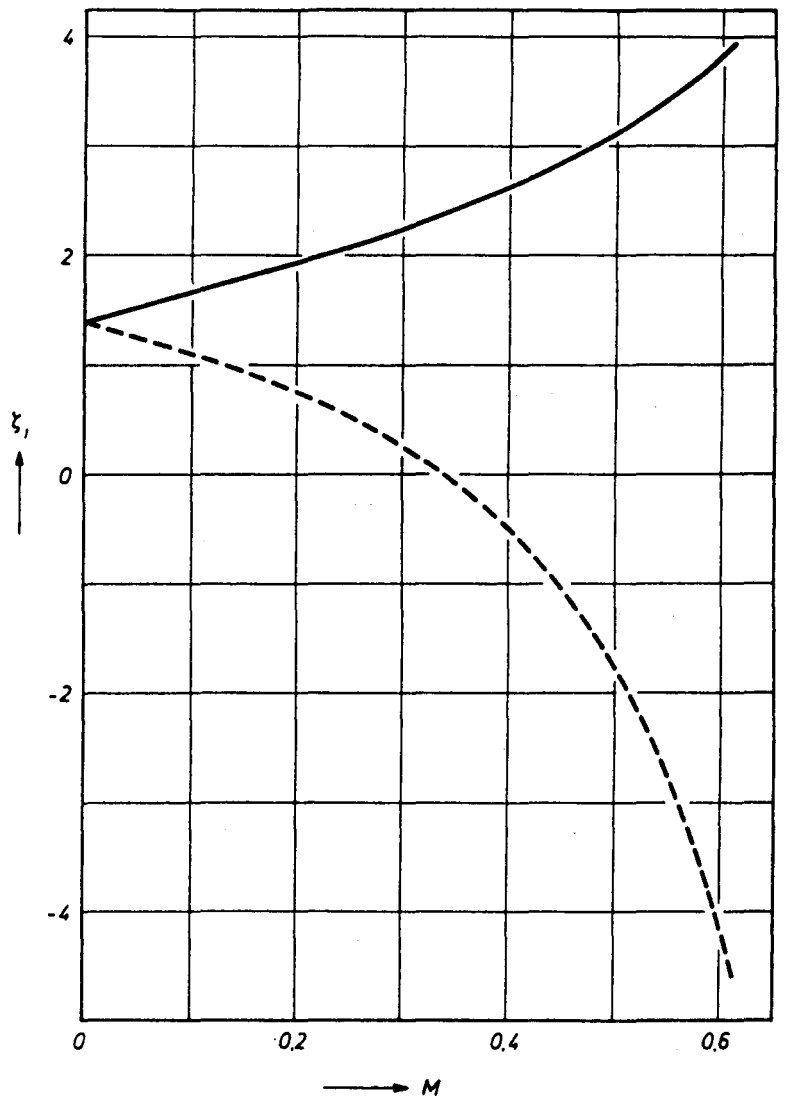

Figure 3.3: $\zeta_1^*(1+M)^4$ as function of M

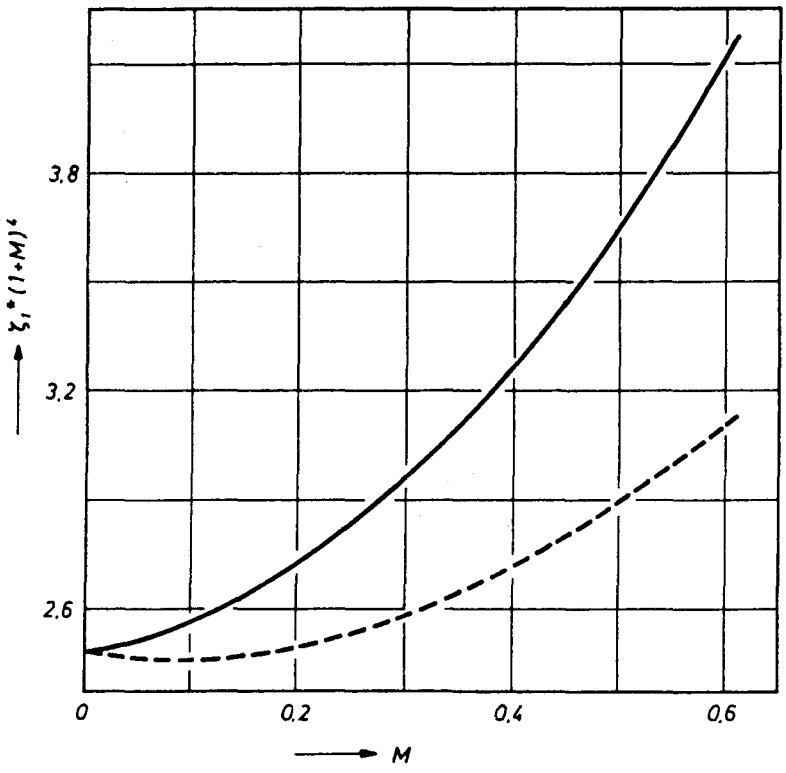

Figure 3.4: ζ_1 as function of M

We will not go any further in describing his theory or the results. We just included this section to introduce the theory of Ronneberger, since it predicts the Doppler effect very well in it's range of validity, for $\delta_v < \delta_l$, as we will see when discussing the measurements.

Chapter 4

Measurement

4.1 Experimental setup

In order to measure the attenuation of plane pressure waves in a long duct, a multiple microphone method is used. The measurement setup is presented in figure 4.1.

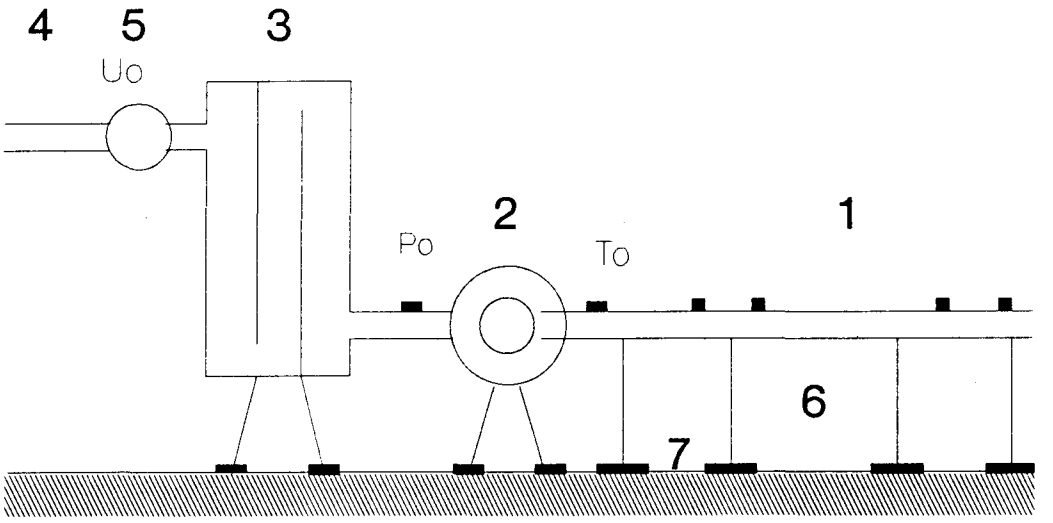

Figure 4.1: The experimental setup
1 microphones; 2 sirene; 3 buffer vessel; 4 dry air supply; 5 turbine meter; 6 pipe; 7 frame

Six acceleration compensated piëzo-electrical pressure probes, type PCB-116A, are mounted upon a long duct. A schematic picture of the mounting of the microphones is given in 4.2. The size of the probes makes a flush mounting impossible. Therefore, they are placed in a small cavity connected with the fluid in the pipe by a small channel. The form of this construction is of general importance, since when making the cavities to small, viscous effects will alter the behaviour of the probe, whereas to big cavities will disturbe the pressure waves in the pipe. The effect of the cavities on the

pressure response of the probes is minimized by a calibration procedure, see [HUI 92].

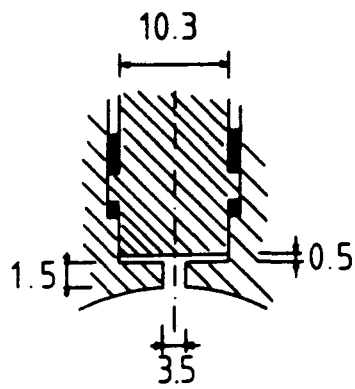

Figure 4.2: The mounting of the microphones

The duct of about 7 m, with an inner radius of $a = 0.015$ m, consists of several pieces. It is therefore possible to reassemble the duct to the alter the length or to change the positions of the microphones. The inner wall roughness is about $\epsilon = 0.1$ μm, and therefore the duct can be regarded as hydraulicly smooth within our range of measurements. The duct ends in a large room (2000 m^3), minimizing the effect of external acoustical fields.

The signal from the microphones is amplified by charge amplifiers (Kistler type 5007/8), which tranform the charge delivered by the piezo-electrical microphones into a voltage. The charge amplifiers are equipped with a low-pass internal filter with a cutoff frequency of 22 KHz. By using the leak resistor of the charge amplifier in the position medium, frequencies below approximatly 0.1 Hz are also cut off.

The resulting signal delivered by the amplifiers is used as input for a data acquisition unit, the HP3565S. This unit is able to perform real-time Fast Fourier Transformation on the pressure signals. This data acquisition unit is controlled by a micro computer (HP9000/360), which is also used to present and store the data collected by the acquisition unit. From there, the data is transfered to an IBM compatible personal computer, to perform the necessary calculations to determine the attenuation of the sound wave.

The sound field is produced by a sirene at the entrance of the duct, driven by an electromotor. The sirene consists of a rotating disc with holes in it, through which the dry air (dew-point -40 .°C), supplied by the buffer vessel (60 bar.) flows. The frequency of the sirene is controlled and tuned by an electronical motor control unit. The frequency can be varied, depending on the number of holes in the disk, in the range 5 Hz to 1 kHz. The frequency fluctuations, limiting the coherent measurement time and the accuracy of the measured transfer functions, are of the order of 0.1 Hz.

The amplitude of the pressure variations in the flow leaving the sirene can be lowered by allowing a part of the air to bypass the rotating disc and mix with the chopped flow. The pressure in the buffer vessel placed directly in front of the sirene is maintained constant by a high pressure pipe-system.

In order to calculate the mean flow velocity U_0 in the duct, the air flowing into the buffer vessel is measured by a turbine meter. The pressure and temperature at the turbine meter, as well as the temperature along the duct, is measered to compensate for the decompression of the air when it flows into the duct under atmospheric pressure. The pressure (0-15 Bar), is measured by a conventional bourdon barometer, type Wallace & Tyrmann, whereas the temperatures are measured by PT-100 probes, accurate up to 0.1 .°C. Also, the speed of sound in dry air c_0 is determined from this temperature measurement using tables of measured data on c_0, as function of temperature [CRC]. This results in an accuracy in the Machnumber $M = U_0/c_0$ of about 1%, which has been checked by measurements on the maximum velocity on the center line of the pipe flow with a Pitot tube [BAL 92], assuming the validity of the relations given for the maximum and mean velocity by literature [SCH 79]. M can be varied in the range of $0 \leq M < 0.3$.

Different pipe terminations can be connected to the duct, in order to change the reflected part of the sound wave, and therefore the ratio of the amplitudes of the up- and downstream sound wave. The circular flare is one of great usefullness, since it has a strong reflection coefficient , giving the reflected wave enough power to be accurately measured.

In order to measure the attenuation in the absence of a mean flow, the duct can be closed at the termination, whereas between the exit of the sirene and the beginning of the duct, a gap of about 5-50 mm allows the air to escape.

4.2 Determination of the attenuation coefficient

As we've seen, the pressure perturbation for harmonic waves along a pipe can be represented by the following linear equation:

$$P(x,t) = \Re\left[\hat{p}^{+} e^{\,i(k_{+}x - \omega t)} + \hat{p}^{-} e^{\,i(-k_{-}x - \omega t)}\right] \tag{4.1}$$

k generally complex. In this equation, the oscillations are represented by $e^{-i\omega t}$, just as in the chapter about the theory of attenuation. This makes it easy to compare theory with some references.

In experimental situations however, we aren't dealing with harmonic waves. Therefore, Fast Fourier Transformation is used as a tool to provide us the information about the harmonic waves in which the signal can be decomposed. The data acquisition unit performing the F.F.T. uses another convention to represent the oscillations, the $+i\omega t$ convention. This means, in order to achieve consistency, that we should write:

$$P(x,t) = \Re\left[\hat{p}^{+} e^{\,i(-k_{+}x + i\omega t)} + \hat{p}^{-} e^{\,i(+k_{-}x + i\omega t)}\right] \tag{4.2}$$

or, relative to the pressure at some position x_{ref},

$$P(x,t) = \Re\left[\hat{p}^{+}(x_{ref}) e^{\,i(-k_{+}(x - x_{ref}) + \omega t)} + \hat{p}^{-}(x_{ref}) e^{\,i(+k_{-}(x - x_{ref}) + \omega t)}\right]$$

The information about the pressure signals from the different microphones is given in the form of transfer functions, describing the linear dependency between the signals. The transfer function H_{21} is defined as:

$$H(\omega)_{21} = \frac{P(x_1,\omega)}{P(x_2,\omega)} \tag{4.3}$$

in which the time dependency has dropped out. $P(x_i,\omega)$ is the fourier component of the pressure wave with frequency ω, measured at position x_i.

Since we know that the attenuation is different for waves traveling in the up- and downstream direction, we want to seperate the pressure amplitudes of the two waves. Therefore, it is convenient to define a pressure reflection

coefficient $R(x_{ref},\omega)$, being the ratio of those complex amplitudes at some position x_{ref}:

$$R(x_{ref},\omega) = \frac{\hat{p}(x_{ref},\omega)_-}{\hat{p}(x_{ref},\omega)_+} \tag{4.4}$$

This reflection coefficient can be expressed in terms of the transfer function, and for the special case of $x_{ref} = x_1$ we get [HUI 92]

$$R(x_1,\omega) = \frac{H_{21} - e^{-ik_+\Delta x}}{e^{ik_-\Delta x} - H_{21}} \tag{4.5}$$

$$\text{with: } \Delta x = x_2 - x_1 \tag{4.6}$$

This enables us to write for the total pressure

$$P(x_1) = p^+(x_1) + p^-(x_1) = p^+(x_1)[1 + R(x_1)] \tag{4.7}$$

giving for the compositing parts

$$p^+(x_1) = \frac{P(x_1)}{1 + R(x_1)} \tag{4.8}$$

$$p^-(x_1) = R(x_1)p^+(x_1) = \frac{P(x_1)R(x_1)}{1 + R(x_1)} \tag{4.9}$$

So, if the complex wavenumber k is known, the reflection coefficient, and therefore the relative amplitudes of the up- and downstream waves at some position x_1 can be determined by measuring the transfer function for a microphone placed at x_1 and an other microphone.

The problem is, however, that we do not know the wavenumber exactly, since we want to measure the small deviations from the wavenumber for free space plane waves due to the acoustical boundary layers! But, when the other microphone is placed relatively close to x_1, the errors in the amplitudes will be small if the approximate wavenumber is used:

$$k_\pm \approx \pm\frac{\omega}{c_0}\frac{1}{1 \pm M} \tag{4.10}$$

Now, in order to determine the wavenumber more exactly, and thereby the small attenuation factor $\pm\alpha_\pm$, the following procedure is used. The

amplitudes $p^+(x_1)$ and $p^-(x_1)$ are determined by two microphones at the beginning of the duct, placed relatively close to each other at x_1 and x_2, as imposed by the reasons mentioned above. The same is done at the other end of the duct, with a second pair of microphones at positions x_3 and x_4. Now, by having the complex amplitudes of the waves at two, distant positions x_1 and x_3, we can calculate the wavenumber by means of the following equation:

$$\frac{p^{\pm}(x_3)}{p^{\pm}(x_1)} = \frac{\hat{p}^{\pm} e^{\mp i k_{\pm} x_3}}{\hat{p}^{\pm} e^{\mp i k_{\pm} x_1}} = e^{\mp i k_{\pm} \Delta x} \tag{4.11}$$

so,

$$k_{\pm} = \frac{\pm i}{\Delta x} \ln \frac{p^{\pm}(x_3)}{p^{\pm}(x_1)} = \frac{\pm i}{\Delta x} \left(\ln \left| \frac{p^{\pm}(x_3)}{p^{\pm}(x_1)} \right| + i \left[\Phi \left(\frac{p^{\pm}(x_3)}{p^{\pm}(x_1)} \right) + 2n\pi \right] \right) \tag{4.12}$$

Since we're considering complex amplitudes, some thougth is to be given on taking the logarithm of a complex quantity. Because each time the wave has made one circle in the complex plane, the cut in the complex plane is crossed, we will loose information on the angle of the quantity $\Phi(Q)$, resulting in an unknown factor $2n\pi i$. The real part of k can however be estimated by $i\omega\Delta x/c_0(1 \pm M)$, since the effect of the attenuation on k will be very small. So by rounding of the difference of the last term of (4.12) with the estimate on $\Re(k)$ to $2n\pi$, we can determine n.

Now, we're able to determine the wavenumber k, based on the calculation of the reflection coefficient with use of the approximate wavenumber $k = i\omega\Delta x/c_0(1 \pm M)$. It is obvious to use this new wavenumber as an improved estimate to recalculate the reflection, in order to get an even better approximation. By repeating this procedure until no improvement is noticable, we can determine the wavenumber k, and thereby the attenuation α. Convergence of the iteration procedure is usually obtained rapidly (five steps are sufficient to achieve a convergence of k and α of order $O(10^-5)$).

It should be mentioned that other methods of determining k with use of the transfer functions can be used. The method we used however, has an important feature. The amplitudes $p^{\pm}$ are determined by local parameters only, and therefore the errors resulting from extrapolition over long distances with use of parameters which can vary over that distance, for example the speed of sound c_0, are minimized. Then, by knowing the up- and downstream wave at two distant positions, the complex wave number can be determined

using the average speed of sound over that distance, removing the need to extrapolate.

In fact, we didn't use four microphones, but six, clustered in two groups. This gave us the opportunity to get independent results for the different possible choices of the four microphones, improving the reliability of the measurements.

4.3 Measurement results

We've measured the sound propagation and attenuation with a multiple microphone method. In principle, the problem is that of the determination of a solution to an over-determined system of lineair equations. This can be done by regression analysis. But, for the sake of simplicity, and to keep contact with the underlying problems, we've choosen data of several combinations of microphones, each time forming a closed set of equations to be solved. The resulting solutions for one measurement are then simply averaged, after being disposed of the unreliable solutions.

In this way, better insight is obtained in the problems arising for certain conditions, especially important since we're in the development fase of the measurement facility.

4.3.1 measurement for the quiescent case

We will presnt the attenuation as measured in the quiescent case. This measurement is done to check the validity of the Kirchhoff solution, as well as to get an impression of the accuracy of the measurements. In figure 4.3 measurements of the attenuation are plotted, as well as the Kirchhoff estimate.

We know that without flow, the direction of propagation shouldn't have any infuence on the attenuation. In the calculation of the wavenumber of the sound wave, we didn't exclude however the dependence on the direction of propagation. As we can see, both the real and imaginairy parts of the attenuation in both directions are in good agreement, with each other as well as with the Kirchhoff estimate. This enables us to calculate the speed of sound from the measured wavenumber, as shown in figure 4.4.

$$k = \frac{\omega}{c_0} + (1+i)\alpha_0 \tag{4.13}$$

$$c_0 = \frac{\omega}{\Re(k) - \Im(k)} \tag{4.14}$$

For the high frequencies, the agreement with the adiabatic sound speed c_0 is outstanding. We clearly see a drop in the speed of sound c_0 *as calculated* for the lower frequencies.

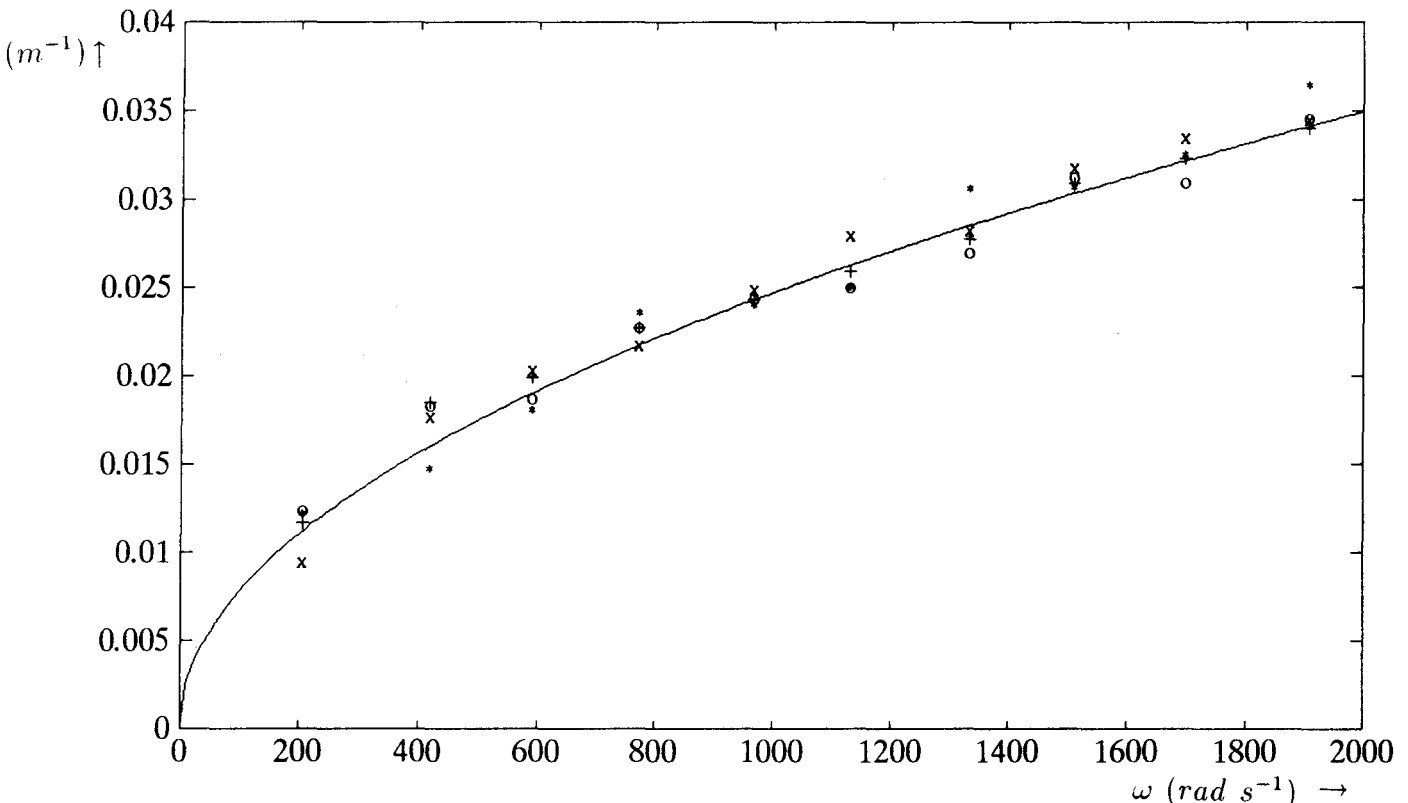

Figure 4.3: Measurement of α (m^{-1}) as function of ω $(rad\ s^{-1})$, no mean flow.
+ $\Im(\alpha_+)$; ∘ $\Im(\alpha_-)$; × $\Re(\alpha_+)$; ∗ $\Re(\alpha_-)$;
— Theory Kirchhoff

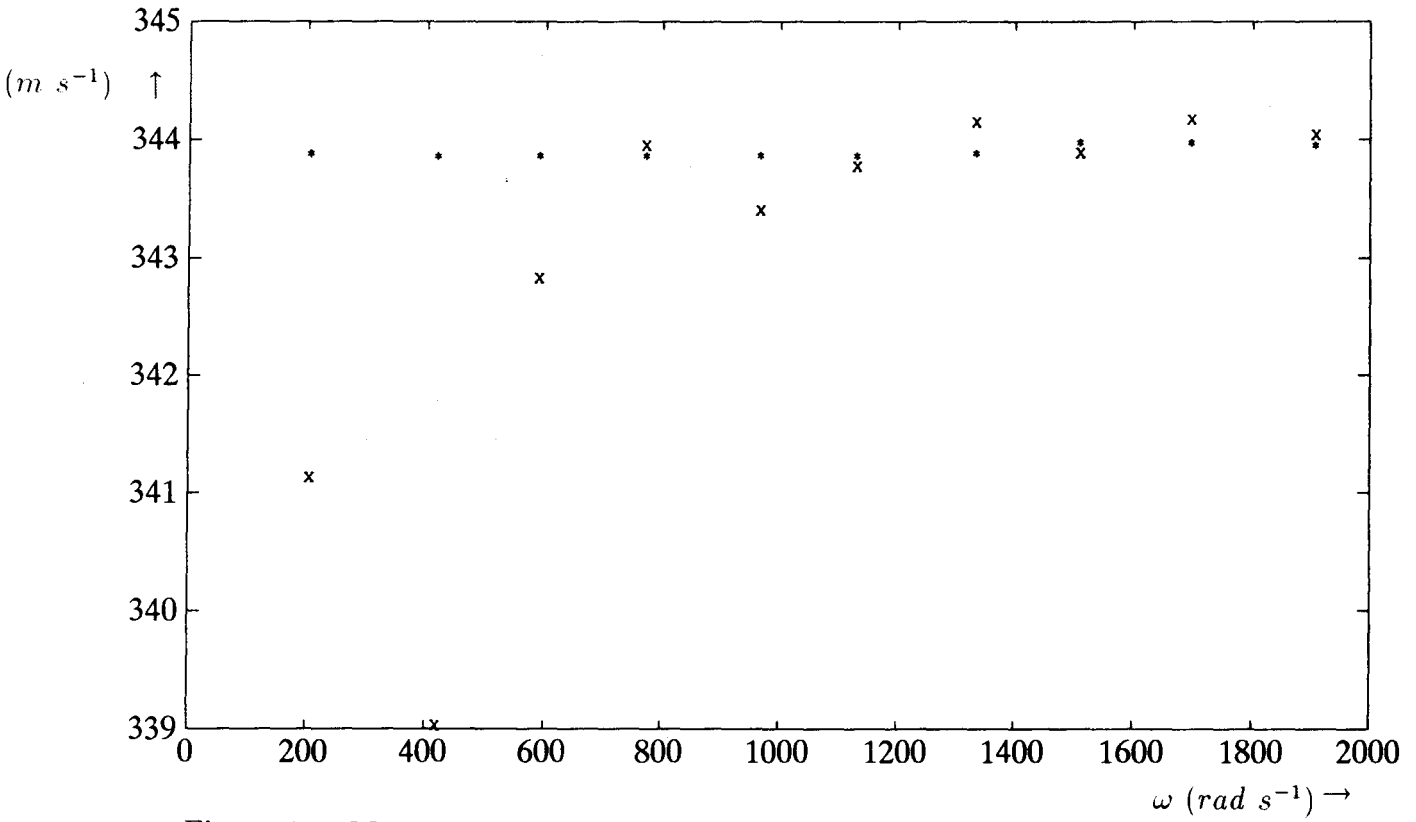

Figure 4.4: Measurement of c $(m\ s^{-1})$ as function of ω $(rad\ s^{-1})$, no mean flow.

$*$ c_0 = adiabatic sound speed; $\times$ $c_{measured}$

4.3.2 measurements with a turbulent mean flow

Before presenting the measurements, let's first take a closer look at the theoretical relation describing the attenuation.

$$\alpha_{\pm} = \pm\left(\frac{1+iA}{(1+M)^2} + \frac{(\gamma-1)(1+iA')}{\sqrt{Pr}}\right)(1+i)\alpha_v \tag{4.15}$$

$$A = A(\delta_v^+);\ A' = A'(\delta_v^+, Pr_t) \tag{4.16}$$

We see, that the effect of the turbulent interactions is described by a dimensionless function of the variable parameters M and δ_v^+. They are not independent, since δ_v^+ is a function of Re, so for one pipe with a fixed radius, a function of M. But since δ_v^+ also depends on the frequency ω of the sound wave, we can choose any combination of δ_v^+ and M, making them effectively independent parameters. So, theoretically speaking, all measurements should fall on one curve when made dimensionless by α_v or α_0 and plotted against M and δ_v^+.

It would be very helpfull for studying the attenuation, if the effects due to the turbulence, possibly depending on the Reynolds number Re, could be seperated from the mean flow effects, determined by the Mach number M. Therefore, two methods can be used to eliminate the Mach dependence, which will be described below.

The factors describing the Mach dependence are different for the viscous and the thermal part of the attenuation, resulting in an unknown Mach dependence if we make no assumptions on the relation between the viscous and thermal contributions to the attenuation. Therefore, a problem arises if we want to determine the form of the functions A and A', or the more commonly used quantities $Z_\tau = (1+iA)(1-i)$ and $Z_q = (1+iA')(1-i)$, also called the normalized wall impedance, since we cannot eliminate the Mach effect from one measurement. This can be overcome by extrapolating several measured values , 'contaminated' by an unknown Mach dependence, to zero Mach number, with respect to a fixed value of δ_v^+.

$$\lim_{M\to 0}^{\delta_v^+ fixed} \frac{\alpha_{\pm}}{i\alpha_0} = \frac{1+i}{i}\frac{1+iA+\frac{\gamma-1}{\sqrt{Pr}}(1+iA')}{1+\frac{\gamma-1}{\sqrt{Pr}}} = \frac{Z_\tau + \frac{\gamma-1}{\sqrt{Pr}}Z_q}{1+\frac{\gamma-1}{\sqrt{Pr}}} = Z_{tot} \tag{4.17}$$

This method, used by Ronneberger and Ahrens [RON 77], has the disadvantage that information about a possible Reynolds-dependence will be lost,

because the Reynolds number is a function of the mean velocity in the pipe U_0 and the radius of the pipe a. Since we used only one pipe, we cannot change U_0 without changing the Reynolds number Re, so by extrapolating the Mach number to zero, the Reynolds number will also vary. Also, the number of measurements must be considerable to make a reliable extrapolation possible.

Therefore, we used an other procedure. We do know the theoretical Mach number dependence in the region of interest, where $\delta_v^+ \gg \delta_l^+$. It is however different for the thermal and viscous impedances, two quantities we do not know. But for $Pr_t = Pr$, thanks to the similarity between heat conduction and momentum transport, expressed in the Prandtl number Pr, the real parts of Z_τ and Z_q, of importance for the Reynolds dependence, are related by:

$$Z_\tau(\delta_v^+) = Z_q(\frac{\delta_v^+}{\sqrt{Pr}}) \tag{4.18}$$

Since we know that Z_τ becomes proportional to δ_v^+, the ratio between the slopes of the impedances will become $\sqrt{Pr}$, assuming Z_τ will not vary to much over a range of $\delta_v^+/\sqrt{Pr}$ to δ_v^+. If we use this approximation, we can eliminate the Mach dependence without extrapolation, keeping the Reynolds dependence unaltered. This is done by summation of the measurements for the up- and downstream direction, and correcting the so obtained 'averaged' value $\overline{\alpha} = (\alpha_+ + \alpha_-)/2$ for the theoretical Mach dependence, and thereby eliminating the Mach dependence.

$$Z_\tau = C\delta_v^+ \Rightarrow Z_q = \frac{C}{\sqrt{Pr}}\delta_v^+ \tag{4.19}$$

$$Z_{tot} = \frac{C\delta_v^+(1+\frac{\gamma-1}{Pr})}{1+\frac{\gamma-1}{\sqrt{Pr}}} \tag{4.20}$$

$$\frac{\overline{\alpha}}{i\alpha_0} = C\delta_v^+ \frac{\left(\frac{1}{2}\left(\frac{1}{(1+M)^2}+\frac{1}{(1-M)^2}\right)+\frac{\gamma-1}{Pr}\right)}{1+\frac{\gamma-1}{\sqrt{Pr}}} \tag{4.21}$$

$$Z_{tot} = \frac{\overline{\alpha}}{i\alpha_0}\left(\frac{1+\frac{\gamma-1}{Pr}}{1+3M^2+\frac{\gamma-1}{Pr}}\right) \tag{4.22}$$

The correction factor is close to unity for low Mach numbers, so a slight error in it due to the theoretical assumptions made above is only of minor influence on the results.

A typical example of the measured attenuation is given in figures 4.5 and 4.6. We see that the scatter for the up- and downstream attenuation is rather large, especially in the low requency region, but the average showes a much more stable behaviour.

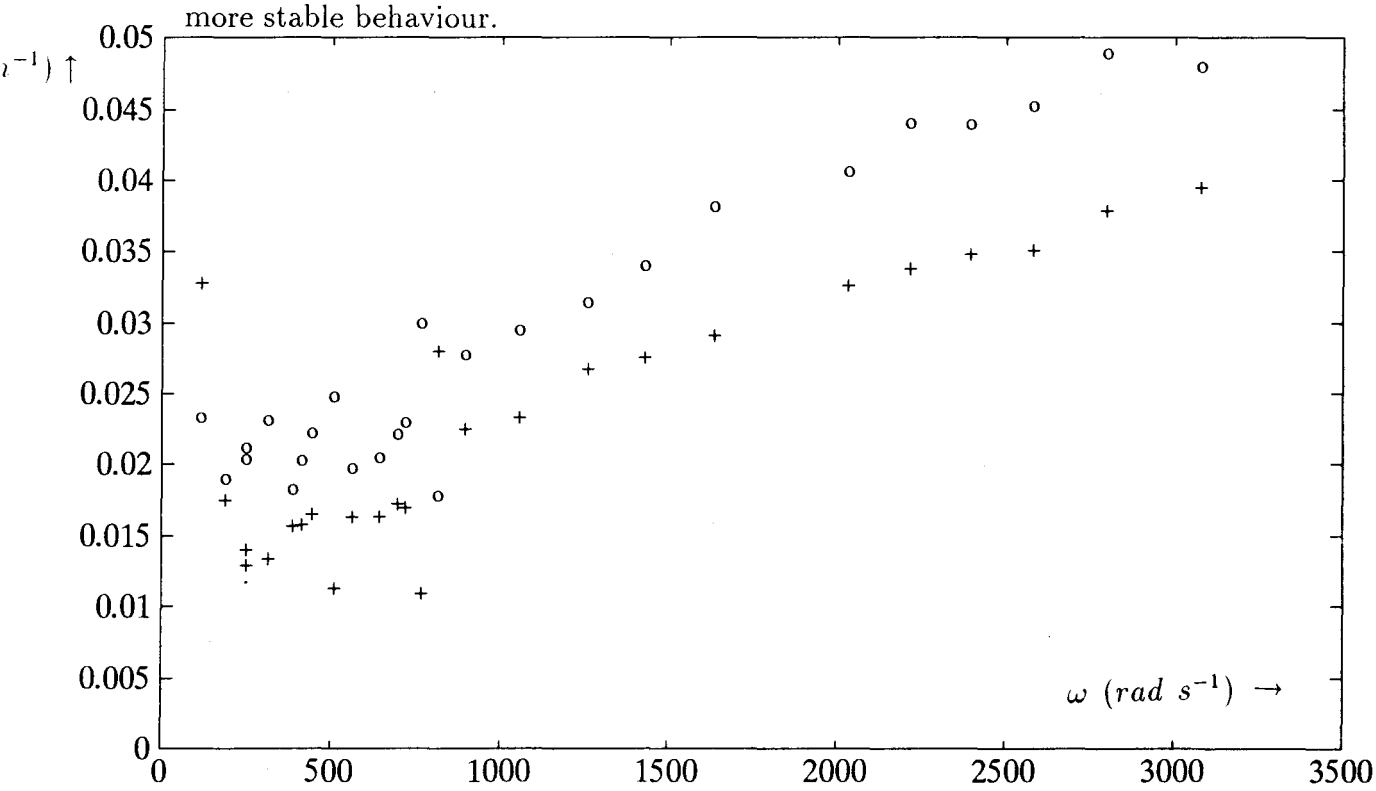

Figure 4.5: Typical measurement of α (m^{-1}) as function of ω $(rad\ s^{-1})$; $M = 0.04$.
$+\ \Im(\alpha_+)$; $\circ\ \Im(\alpha_-)$.

Some check can be made on the assumptions on the Mach dependence, since for the ratio $\Im(\alpha_+)/\Im(\alpha_-)$, the following relation should hold:

$$\frac{\Im(\alpha_+)}{\Im(\alpha_-)} = \frac{\frac{1}{(1+M)^2} + \frac{\gamma-1}{Pr}}{\frac{1}{(1-M)^2} + \frac{\gamma-1}{Pr}} \tag{4.23}$$

The result is shown in the following table, calculated with use of the data in figure 4.7.

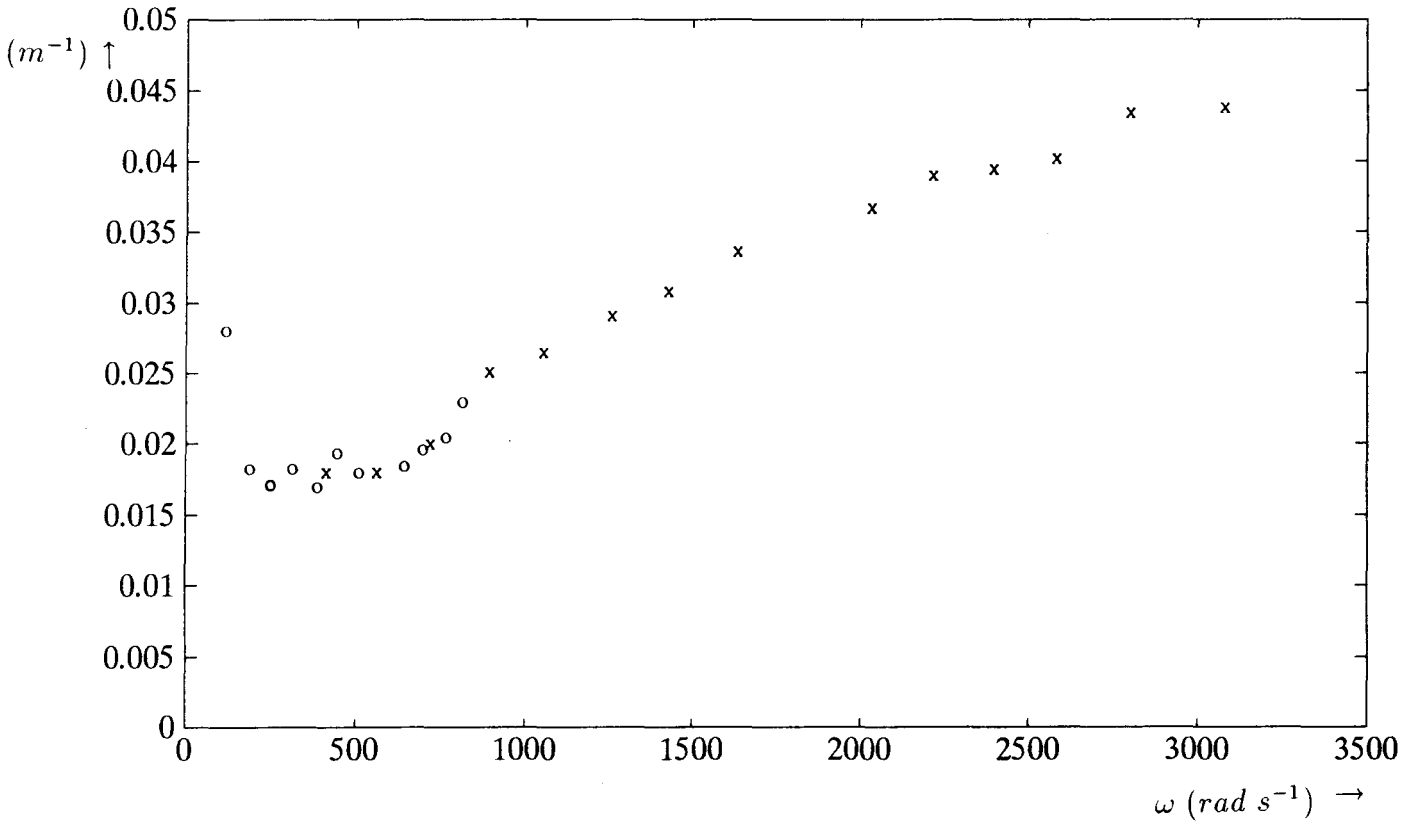

Figure 4.6: The average of up- and downstream parts $\overline{\alpha}$ (m^{-1}) as function of ω $(rad\ s^{-1})$; $M = 0.04$.
o $\Im(\overline{\alpha})$, measurement a
× $\Im(\overline{\alpha})$, measurement b.

M	$\Im(\alpha_+)/\Im(\alpha_-)$	eq.4.23
0.1	1.60	1.30
0.2	1.69	1.69
0.3	2.28	2.26

We can see from it, that for $\delta_v^+ < \delta_l^+$, the Mach dependence is not as we expected, but since the correction factor is close to unity, we will use (4.22) for the whole range of measurements.

The result for Z_{tot} is shown in figure 4.8, in which also measurements made by Ronneberger and Ahrens are plotted, who used the mach extrapolation.

To make a comparison with the stationary limit, we have plotted Z_{tot}/δ_v^+ as function of $(1/\delta_v^+)^2$ for the different measurements in figure 4.9. Only the real part is plotted, since that's the part possibly related to the stationary limit.

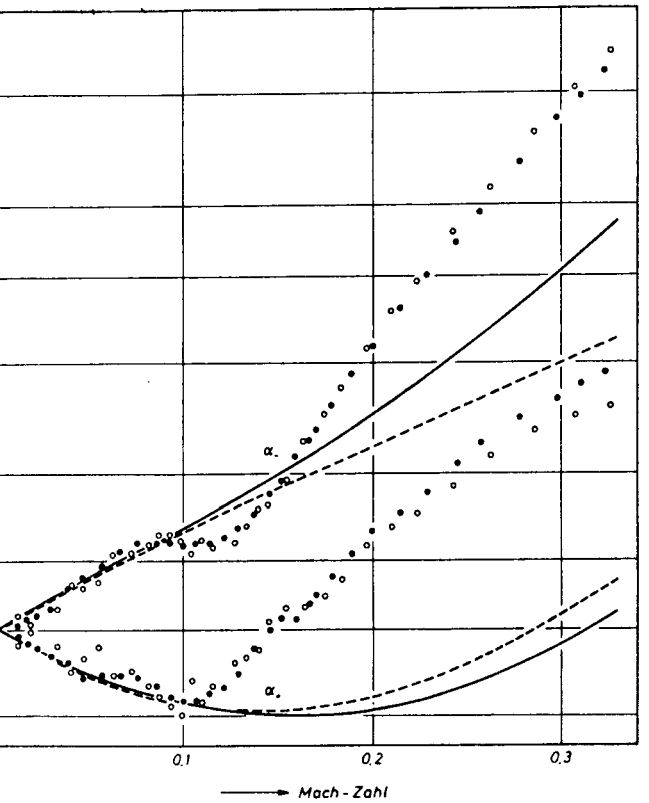

ur 7a Dämpfungskonstanten für Schallausbreitung stromab (α_+) und stromauf (α_-) bei 630 Hz im 20-mm-Rohr
• Meßreihe I, ○ Meßreihe II
—— "Exakte" Rechnung (Abschnitt 2.2.3)
--- Näherungsrechnung (Gleichung (2.60))

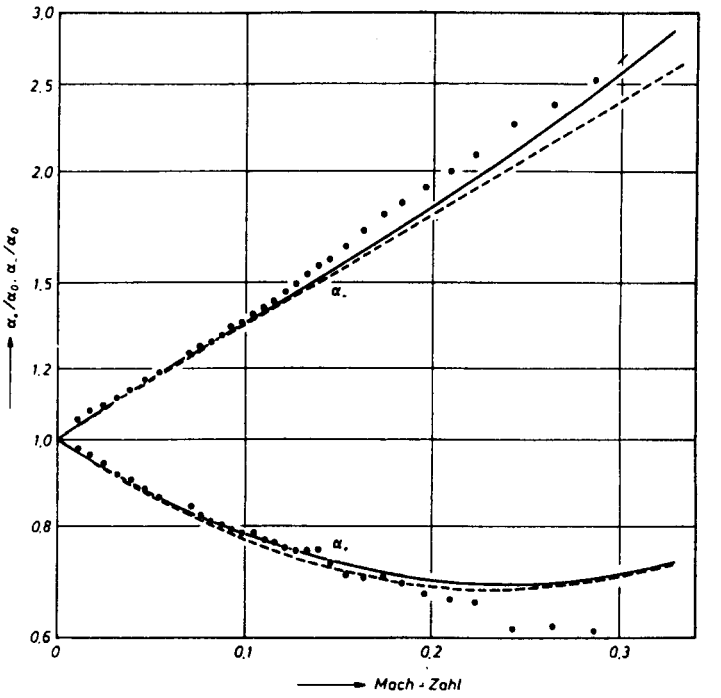

Figur 7b Dämpfungskonstanten für Schallausbreitung stromab (α_+) und stromauf (α_-) bei 3348 Hz im 20-mm-Rohr
—— "Exakte" Rechnung (Abschnitt 2.2.3)
---- Näherungsrechnung (Gleichung (2.60))

Figure 4.7: Measurement of the ratio $\alpha_\pm/i\alpha_0$, as made by Ronneberger and Ahrens

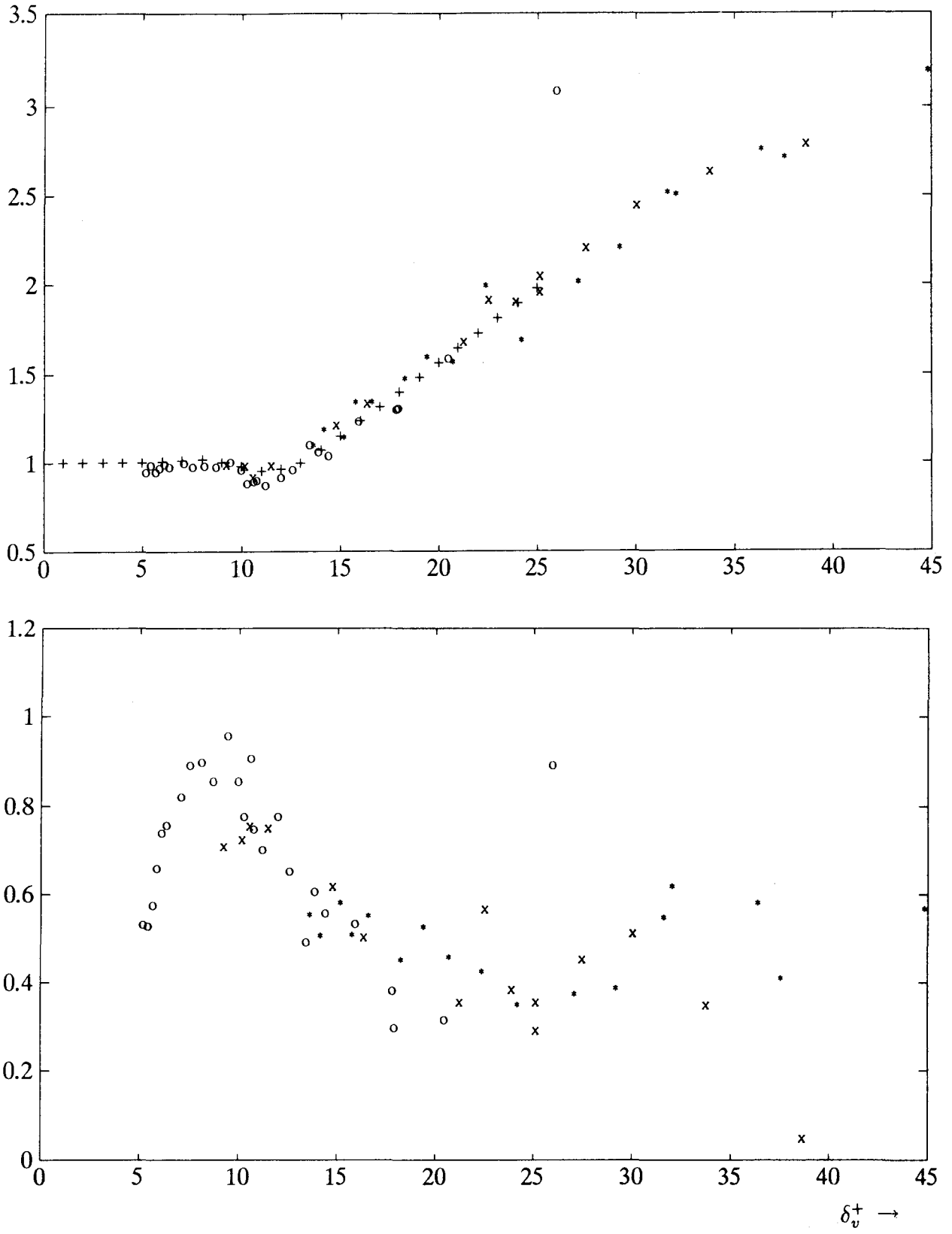

Figure 4.8: Measurement of Z_{tot} as function of δ_v^+
o $Re = 2.7 \cdot 10^4$; $\times$ $Re = 5.3 \cdot 10^4$; $*$ $Re = 8 \cdot 10^4$; + Ronneberger.

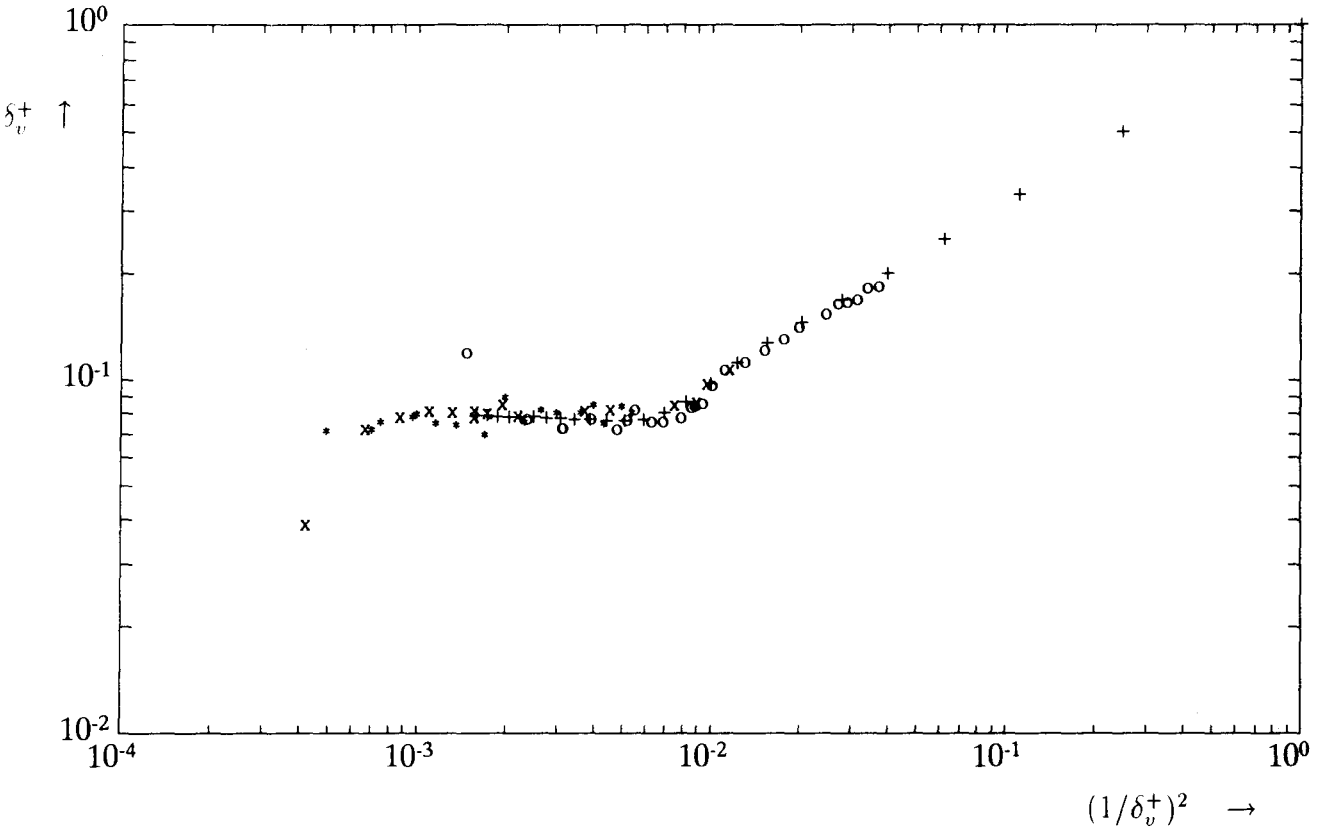

Figure 4.9: Measurement of Z_{tot}/δ_v^+ as function of $(1/\delta_v^+)^2$
o $Re = 2.7 \cdot 10^4$; $\times$ $Re = 5.3 \cdot 10^4$; $*$ $Re = 8 \cdot 10^4$; $+$ Ronneberger.

Chapter 5

discussion

5.1 Quiescent case

As can be seen from the measurements for the quiescent case, the multiple microphone method provides us the possibility to measure the real and imaginairy parts of the attenuation with an accuracy of 5%. This means a maximum accuracy of about $3 \cdot 10^{-4}\%$ in the determination of the real part of the wavenumber of the sound k! Also, the agreement between the up- and downstream attenuation is excellent.

The drop in the calculated speed of sound for low frequencies, is probably a result of the error introduced by using the boundary layer approximation, and not a drop in the actual adiabatic sound speed c_0. For the lower frequencies, the boundary layer becomes so large, that the radius a of the pipe is no longer large compared to the boundary layer thickness δ_v. The attenuation becomes asymmetrical for the real and the imaginairy parts, so $\Re(\alpha)$ is not equal to $\Im(\alpha)$ any more. The result is that the method of calculation of c_0 is no longer valid. An exact solution of the equations on which we based our boundary layer approximations is given by Tijdeman [TIJ 75]. We can conclude from this measurement, that we must be carefull when using very low frequencies, since the boundary layer approximations may not be accurate enough.

5.2 Situation with flow

We've plotted our measurement of Z_{tot} with those of Ronneberger and with the theoretical curves in figure 5.1. When looking at the measured total impedance Z_{tot}, we can distinguish the three typical zones, also found in the theoretical Z_{tot}.

5.2.1 The Kirchhoff limit

We see clearly, that the measurements all go to the theoretical limit of unity for small δ_v^+, so they all tend to the Kirchhoff attenuation, as expected.

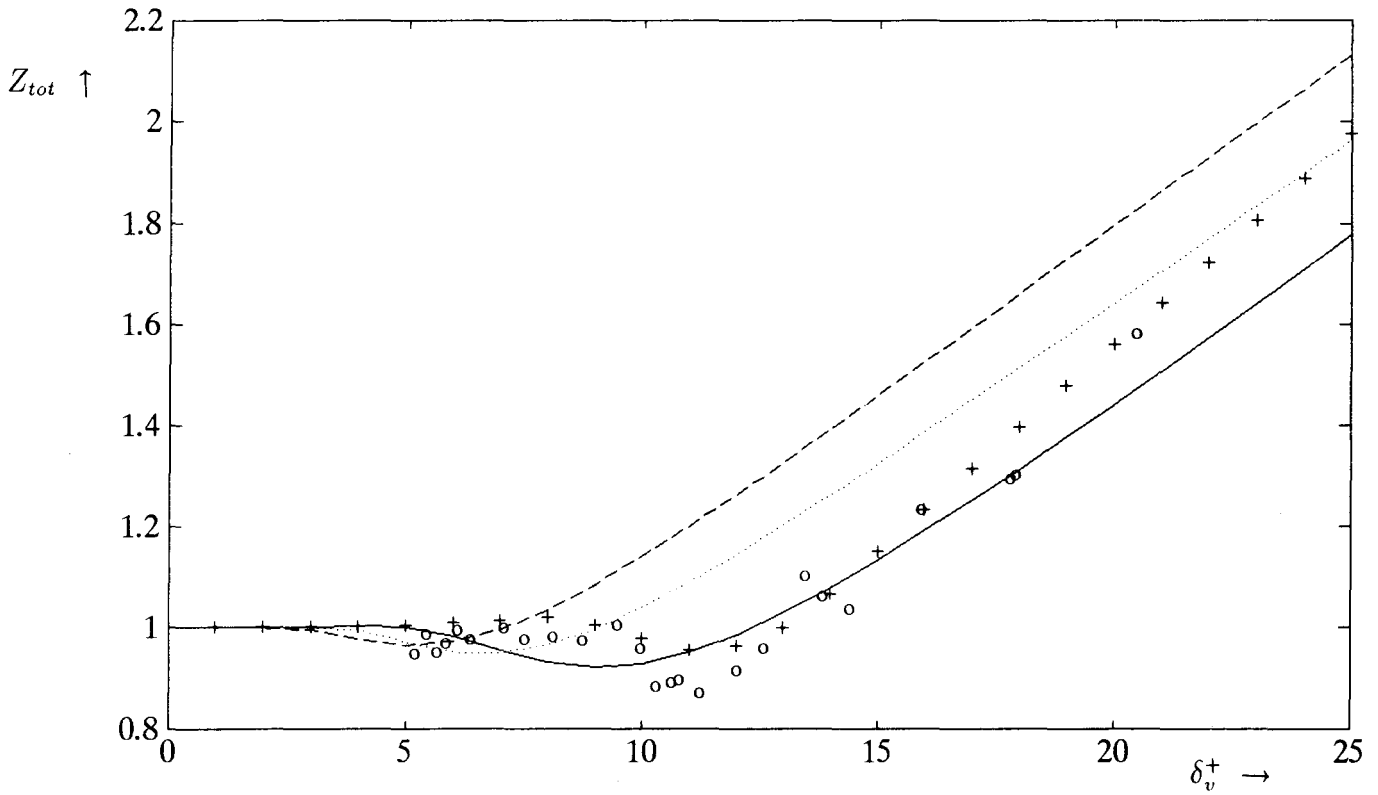

Figure 5.1: Z_{tot} as function of δ_v^+.
o, measurement, $M = 0.04$
+, measurement Ronneberger
—— rigid plate limit ($\delta_l^+ = 15$)
- - - Howe ($y_0^+ = \delta_l^+ = 7$)
· · · new model of η_t ($y_0^+ = 0$; $\delta_l^+ = 10.7$)

5.2.2 The dip

The measured minimum in Z_{tot}, due to the interference of the shear wave with it's reflection on the turbulent zone, is deeper than that measured by Ronneberger, but the place is in agreement. If we compare it with the theoretical curves, we see that value of the minimum as measured by Ronneberger coincides with the value given by the curve for the model of η_t we proposed, but non of the three theories does predict the position of the minimum accurately.

It must be stated, that the measurements of Ronneberger were reconstructed from the values he presented for the impedancies Z_τ and Z_q. He actually measured Z_{tot}, and substracted a Z_q, calculated from measurements on the turbulent heat transport in the absence of sound, and presented it as Z_τ. He did however measure Z_τ also more directly, by an experiment in water. Both measurements agree well, despite the fact, that the Z_q he used, doesn't have the same form as Z_τ, as imposed by the analogy between the heat conduction and momentum transport, as expressed by the Prandtl number Pr.

The dip is thought to be caused by interference of the shear wave with it's reflection at the turbulent zone (see [RON 77]).

One reason for a possible shift of the position of the dip with respect to the calculated position, is an interaction of the shear wave with the apparent viscotity η_t. We could imagine, that the Prandtl mixing length l becomes comparable to the 'wavelength' of the shear wave. If this would occur, the approximations used in deriving the apparent viscosity are no longer valid, as we can see in figure 5.2. We used the approximation:

$$\Delta u \approx l\frac{\partial u}{\partial y} = l(\frac{\partial u_0}{\partial y} + \frac{\partial u'}{\partial y}) \tag{5.1}$$

This approximation will be valid if $l \ll \pi\delta_v$, since then the mixing length l will be less then halve the wavelength of the shear wave, which is defined as:

$$\lambda_{shear} = 2\pi\delta_v \tag{5.2}$$

This wavelength of the shear wave must of course be evaluated for the turbulent region. Since $\delta_v = \sqrt{2\eta/\omega\rho_0}$, we can estimate the wavelength for the turbulent zone by setting $\eta =: \eta_t \leq 2K\delta_l^+\eta$, resulting in a wavelength for the

turbulent zone $\lambda_{shear,t}$ which is at least three times of that in the laminar region. Using the relation $l = Ky$, we come to the relation

$$y \ll \frac{\pi}{K}\delta_{v,turbulent} \approx 8\delta_{v,turbulent} \approx 25\delta_v \tag{5.3}$$

Tresspassing of this condition will not be of influence if the shear wave is damped before reaching the turbulent zone, so for $\delta_v \ll \delta_l$. The same is true if $\delta_v \gg \delta_l$, since then the shear wave will also be damped before y becomes of order $\delta_{v,turbulent}$, because of the decrease in amplitude with height at least exponentially, conform $u' = u'(0)e^{-y/\delta_{v,turbulent}}$. When however δ_l is of the same order as δ_v, the wave hasn't had the chance to damp very much, and the wrong approximation of $\Delta u = l\partial u/\partial y$ is used in a region were the amplitude of the shear wave cannot be neglected, resulting in an error of considerable magnitude.

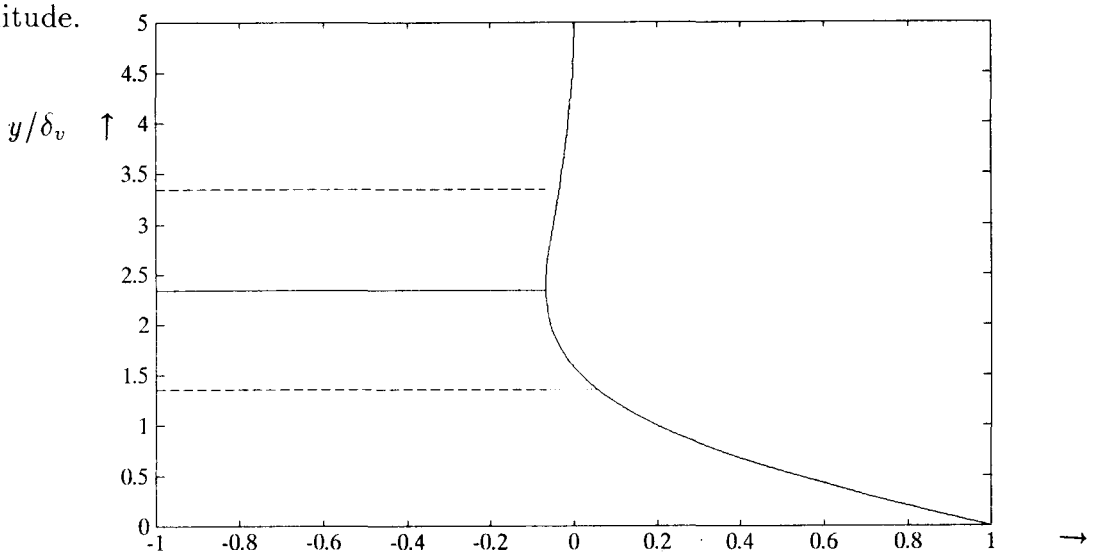

Figure 5.2: Illustration of a possible phase error due to the distance travelled. $u_{bl}/|u_{ac}|$ as function of y/δ_v
$\cdots$ error in the predicted velocity difference

Another reason for this shift in position of the dip could be that during the time that the fluid particle with turbulent velocity in the axial direction travels from one layer to another, causing the transport of momentum, the phase of the destination layer has shifted, as illustrated in figure 5.3. Since the phase of the shear wave changes according to ωt, the limiting condition

becomes $\omega t < \pi$. The time the fluid particle takes, can be calculated by realising that $t = l/u_0 \approx (\partial u_0/\partial y)^{-1} = \eta/\tau_0$. Combining these relation gives as limiting condition:

$$\frac{\omega\eta}{\tau_0} < \pi \tag{5.4}$$

$$\frac{8\omega\eta}{\phi\rho_0 U_0^2} < \pi \tag{5.5}$$

Since ϕ does not change much in the range of Reynolds numbers we're considering, we use the approximate value of $\phi \approx 0.02$, resulting in the condition

$$\omega < 6 \cdot 10^7 (rad\ s^{-1}) M^2 \tag{5.6}$$

This means, that for $M = 0.005$, the maximum radial frequency becomes $\omega < 1500(rad\ s^{-1})$. All our measurements fall within that range, but it shows that we must be carefull when measuring with extremely small Mach numbers.

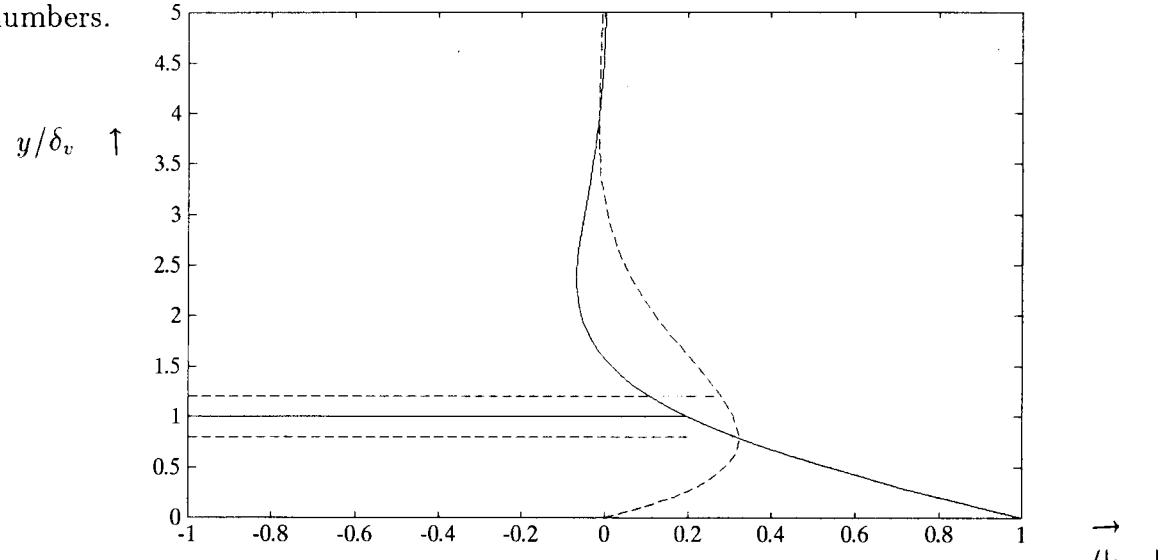

Figure 5.3: Illustration of the possible error due to the time of the journey from one layer to another.
$u_{bl}/|u_{ac}|$ as function of y/δ_v
—— shear wave on $t = 0$
- - - shear wave on $t = \pi/2$
· · · error in the predicted velocity difference.

Correcting both errors described above is essentially the same as introducing a phase lag between the incident and reflected shear wave. We will show that this will shift the calculated position of the dip to the right by examining the behaviour of the rigid plate model (see section 2.4). We have plotted in figure 5.4 the normalized total impedance Z_{tot} as function of δ_v^+, for different values of δ_l^+.

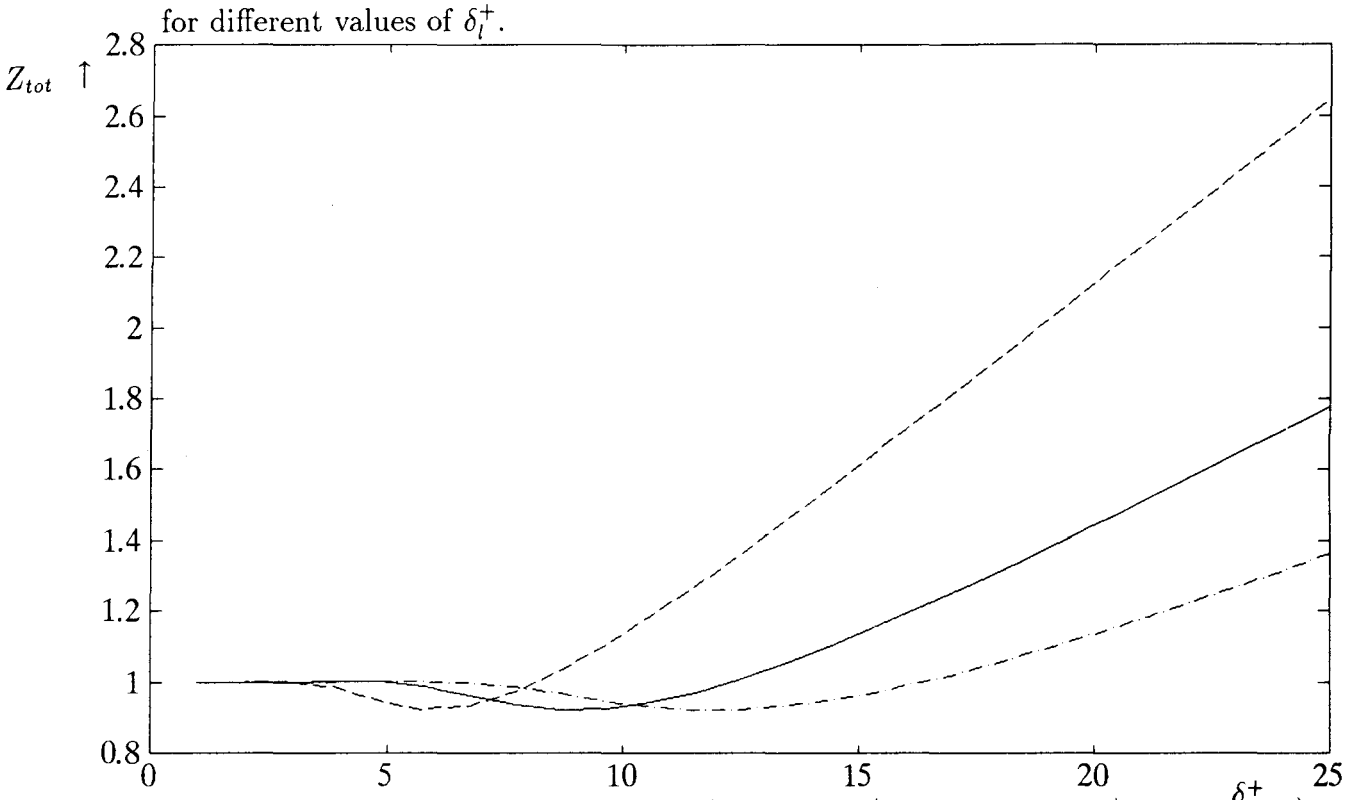

Figure 5.4: Z_{tot} as function of δ_v^+.- - -$\delta_l^+ = 10$ —$\delta_l^+ = 15$ — · — $\delta_l^+ = 20$

As we can see, the dip shifts to the left for increasing δ_l. The minimum (maximum interference) will occur if half the wavelength of the shear wave matches the distance the shear wave travels going from the wall to the edge of the turbulence and back. This implies, using (5.2):

$$\frac{\lambda_{shear}}{2} = 2\delta_l \tag{5.7}$$

$$\delta_v^+ = \frac{2\delta_l^+}{\pi} \tag{5.8}$$

The position of the minimum as observed in the measurements, could be

explained as a result of a phase lag of the reflected wave. The actual distance where the reflection occurs, determining the depth of the minimum, is then combined by the virtual distance of the node of the wave, determined by the phase lag. This results in a position of the dip on the right side of the position determined by the actual edge of the turbulent zone. So, the position of the dip calculated with for example $\delta_l^+ = 15$, could be shifted due to this phase lag to a position in accordance with the calculated position for $\delta_l^+ = 20$. As we can see in figure 5.4, this minimum will then shift to the right.

A reason for lowering of the dip might be the caused by the fact that the turbulence time scale becomes comparable to the time scale of the sound wave. The quasisteady approach then becomes questionable. The conditions for which these time-scales become comparable, can be estimated by the following argumentation.

The maximum dimension of the turbulent structures is the diameter of the pipe, $2a$. If we realise that these structures travel with the velocity of the mean flow, we can estimate the frequency of these turbulent motions with respect to a fixed position in the pipe. We get $f_{turb} = U_0/2a$, or, expressed in the radial frequency, $\omega_{turb} = \pi U_0/a$. If we compare this frequency ω_{turb} with the frequency of the sound waves ω_{ac}, we get the Strouhal number, $Sr = \omega_{turb}/\omega_{ac} = \pi U_0/a\omega_{ac}$. If we calculate for which frequency the Strouhal number becomes of order $O(1)$, for a typical value of the mean flow velocity of $U_0 = 13\ m/s$, $(M = 0.04)$ and a pipe radius of $0.015\ m$, we get:

$$\omega_{ac} \approx 3000\ (rad/s) \tag{5.9}$$

This is also the maximum frequency we used in our experiments. We see however , that the assumption of quasisteady behaviour of the acoustical disturbances must be kept in mind. It could be a reason for a possible Strouhal number dependence of the attenuation, especially for values of $\delta_v > \delta_l$.

5.2.3 The static limit

For determining the behaviour of Z_{tot} for large δ_v^+, we've plotted Z_τ/δ_v^+ as function of $(1/\delta_v^+)^2$. In figure 5.5, we've drawn the lines determined by the static limit for the different measurements. As we can see, All measurements are on the line corresponding to the measurement with the lowest Reynolds

number. More important is, that the measurements show no Reynolds dependence, at least not within the measuring range.

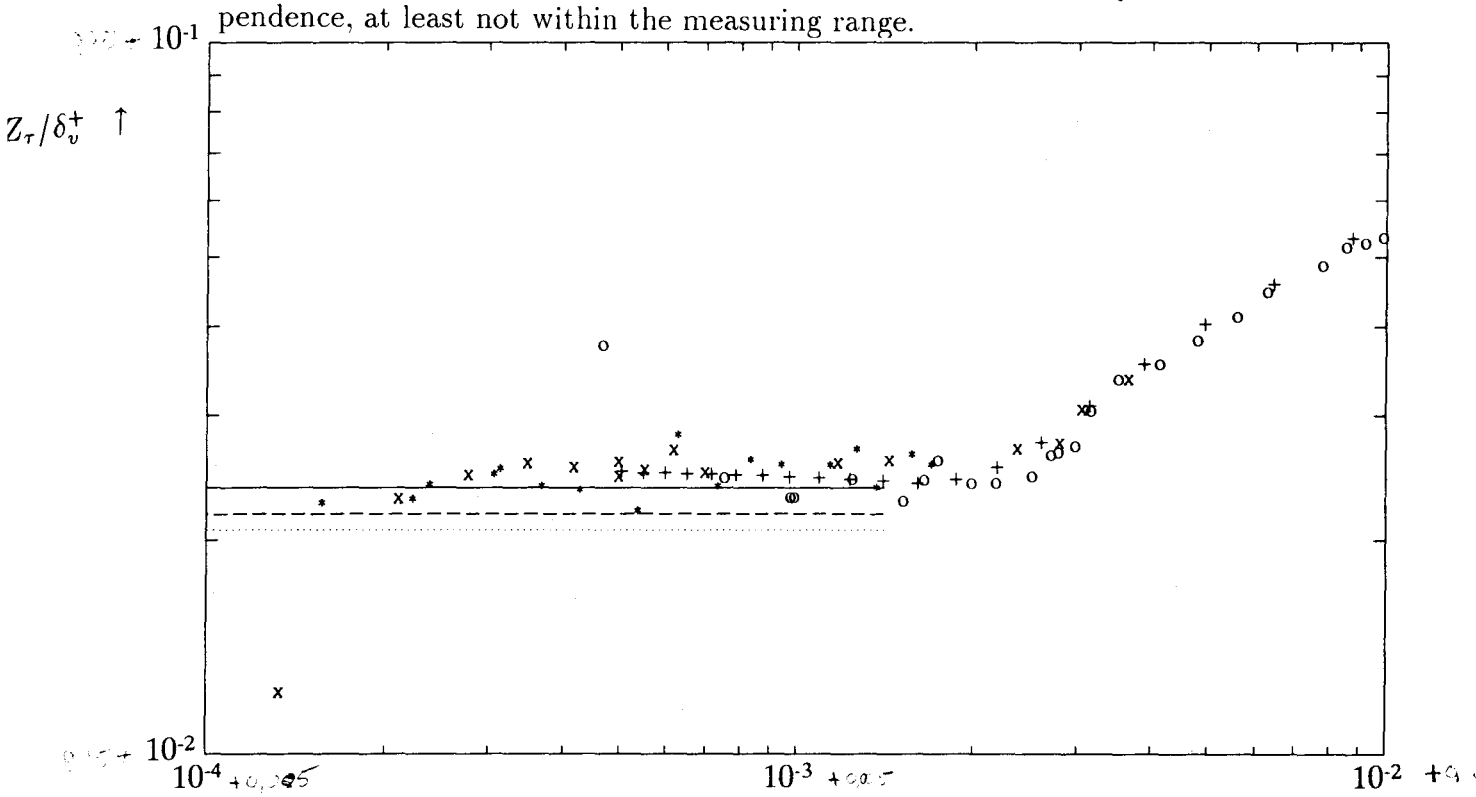

Figure 5.5: Z_{tot}/δ_v^+ as function of $(1/\delta_v^+)^2$.
o $Re = 2.7 \cdot 10^{-4}$; × $Re = 5.3 \cdot 10^{-4}$; ∗ $Re = 8 \cdot 10^{-4}$; + Ronneberger.
—— static limit $Re = 2.7 \cdot 10^4$
- - - static limit $Re = 5.3 \cdot 10^4$
· · · static limit $Re = 8 \cdot 10^4$

When plotting the theories using an apparent viscosity with the data, as in figure 5.6, we see that in the upper right corner of the figure, the theoretical curves converge into a straight line, corresponding to the limiting value $Z_{tot} = 1$ for small δ_v^+. We already saw that the measured data also tends to this limit.

When looking at the other limit, for small values of the parameter $(1/\delta_v^+)^2$, we also see the three theories converging. They will start to diverge however when they have passed the point of convergence, although very slowly. Both the theories with a finite estimate on η_t will continue to lower, while the rigid plate theory asymptotically attains the value $1/\delta_l^+$. The most important fea-

ture is, that non of them shows a Reynolds dependence. The measurements are in good agreement with the theoretical curves. This is achieved for the rigid plate model by changing the empirical value of $\delta_l^+ = 10.7$ to $\delta_l^+{}_{rp} = 15$. For the model of Howe, the same is done, resulting in a value of $\delta_l^+{}_{Howe} = 7$. The new model does well without changing the empirical value of $\delta_l^+ = 10.7$.

Because of the scatter in the data, no definite judgement on the models can be made, but there is a slight favor for the models using a finite apparent viscosity η_t.

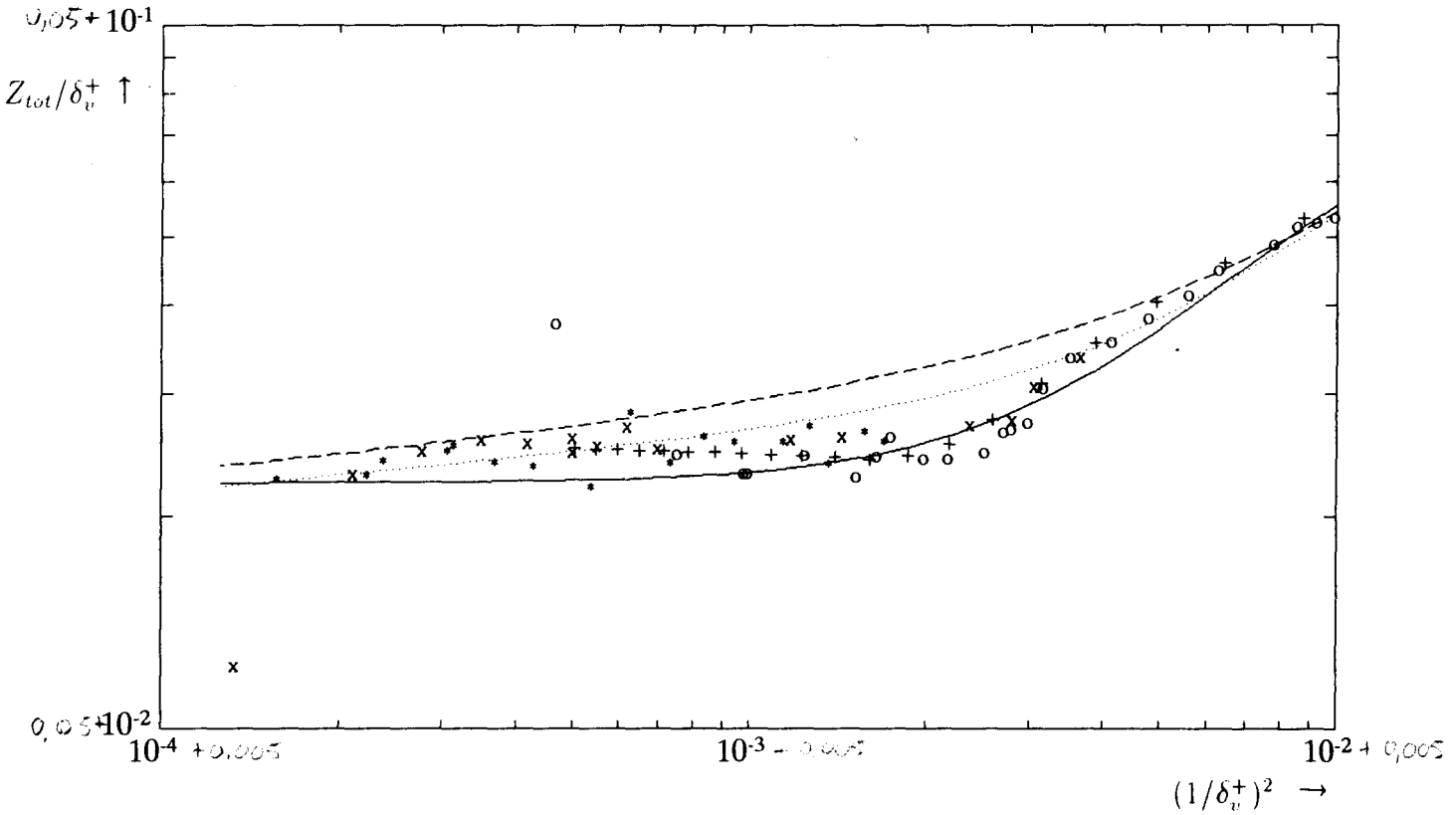

Figure 5.6: Z_{tot}/δ_v^+ as function of $(1/\delta_v^+)^2$.
o $Re = 2.7 \cdot 10^4$; × $Re = 5.3 \cdot 10^4$; ∗ $Re = 8 \cdot 10^4$; + Ronneberger.
—— rigid plate limit ($\delta_l^+ = 15$)
- - - Howe ($y_0^+ = \delta_l^+ = 7$)
· · · new model of η_t ($y_0^+ = 0$; $\delta_l^+ = 10.7$)

The absence of a Reynolds dependence in the theories is the result of using a 2-dimensional theory with infinitive dimensions of the boundary layers. Therefore, the radius of the pipe has ceased to be of importance in determining the attenuation.

There is however a lower limit to the validity of the theories, since we've used the 2-dimensional equations in determining the expressions for the boundary layers. To be valid, the ratio δ_v/a must be small. When setting an arbitrary limit of 10% for this ratio, we come in our experimental setup to a maximum of $\delta_v < 1.5 \cdot 10^{-3} m$ corresponding to a radial frequency of $\omega > 10 rads^{-1}$.

We can now determine the maximum value of δ_v^+, after which the theory ceases to be valid, for the three different Reynold numbers at which we measured. The results are printed in the following table:

$Re\ (\cdot 10^4)$	δ_v+_{max}	$(1/\delta_v+_{max})^2\ (\cdot 10^{-5})$
2.7	75	18.0
5.3	135	5.3
8.0	195	2.6

These values are of the same order as the actual positions of the crossings of the theoretical curves for the turbulency theories with those determined from the stationary theory.

Chapter 6

Conclusions and recommendations

6.1 Conclusions

We've found that the multiple microphone method can be used to determine the attenuation of plane waves in a pipe. In the quiescent case the agreement between theory and experiment is outstanding, for the real and imaginairy parts of the opposite directions of propagation, indicating that the method is accurate enough to measure the attenuation in the case of a fully developped turbulent mean flow in a hydraulicly smooth pipe.

The measurements that where performed for the case of a turbulent mean flow show some interesting features. Two parameters turn out to be of importance in the determination of the attenuation, being δ_v+ and δ_l^+, representing the dimensionless thicknesses of the viscous (acoustical) and laminar (turbulent) boundary layers. In our experimental setup, the thickness of the laminar boundary layer is determined by the choice of Re, equivalent to the choice of M or U_0, whereas the thickness of the oscillating viscous sublayer, also called the shear wave, is determined by w. They together determine completely the form of the dimensionless total impedance of the sound wave Z_{tot}, which is closely related to the attenuation.

These parameters divide Z_{tot} essentially in three regions, $\delta_v+ \ll \delta_l^+$, $\delta_v^+ \approx \delta_l^+$ and $\delta_v^+ \gg \delta_l^+$. In the first region, the attenuation is actually described by the Kirchhoff estimate, which also is found as a limiting case of the models based on an apparent turbulent viscosity η_t.

In the second area, a strong minimum in Z_{tot} is found, being the result of interference of the shear wave with it's reflections at the turbulent region. The theories do predict such a minimum, but neither of them is at the right place. The depth of the dip as measured by Ronneberger is in agreement with the depth of the new model on the turbulent viscosity, but only for the case of the measurements in air. The error in the depth of the dip might be due to interference of the shear wave with the mixing length hypothesis.

In the thirth region, the attenuation is either determined by the elevation of the function Z_{tot} as function of δ_v^+, or by the static limit directly deduced from the linearisation of small disturbances of the stationary turbulent flow. The first option implies that there is no dependence of the attenuation on the Reynolds number, whereas the second implies that there is such a dependency and a limiting value. The measurements don't reach far enough to make a definite judgement on this, but there's no indication of a Reynolds dependence in our present measurements.

It is however quite surprising that when calculating the maximum value of δ_v^+ for which the theories based on the apparent viscosity remain valid, the corresponding limiting value of the elevation of Z_{tot} is in agreement with the static limit. This is a strong indication that the static limit may determine the behaviour beyond the validity of these theories, effectively re-introducing a Reynolds dependency. This Reynolds dependency was essentially lost due to the use of a 2-dimensional approximation for the boundary layer equations, neglecting the finite dimension of the pipe, being the radius a.

Another important conclusion is, that the new model for the apparent turbulent viscosity η_t, fits the data as well as the other theories, but uses a value for the dimensionless thickness $\delta_l^+ = 10.7$, which is in agreement with the value found from the semi-empirical theory of fully developped stationary turbulent pipe flow. This gives us the possibility to expand it's use to completely rough pipes, we're the turbulent profile is not determined by the thickness of the laminar boundary layer, but by the height of the protrusions. This is of course of major importance for industrial applications of the theory.

6.2 recommendations

As can be read in the conclusions, some questions are not answered yet. Some answers can only be given when further measurements are made, expanding the range of measurements mainly towards the lower values of δ_v^+. Then we can determine if the Reynolds dependency occurs for this region, and if the validity of the models is maintained in that region. The measurements must be done systematically, which is possible since we've found the two parameters of interest.

An interesting option for expanding the range of measurements, is to increase the mean pressure, and thereby the density ρ_0 of the fluid. Since $\delta_v = \sqrt{2\eta/\omega\rho_0}$ depends on the density, and δ_l is approximately proportional to $\eta/\rho_0 U_0$, we see that we can alter the ratio δ_v/δ_l proportional to $\sqrt{\rho_0}$.

Also, measurements on rough pipes can be very interesting, to check if the new theory holds for that case. Thourough investigations must be made, to determine the sort of roughness and the characteristic height of the protrusions to be used to get interesting results.

On the theoretical side, attemps could be made to include the dimensions

of the pipe, re-introducing the Reynolds dependency. This can be done in several degrees. The most easy introduction is possibly to perform the integration of the boundary layer in radial coordinates, just as was done for the case of stationary turbulent flow.

Second, the boundary conditions could be imposed at the middle of the pipe, instead of using infinitive boundary layers. One could attempt to solve the entire equations for the axial coordinates, but this will probably introduce unsolvable problems for analytical treatment.

The possible coupling of the Prandtl mixing length with the shear wave must thouroughly be investigated. The use of a second order approximation in the determination of the turbulent velocities could be a solution.

Also, the Mach dependency for the low values of δ_v^+ predicted by the turbulent viscosity models is not right, whereas the quasilaminar theory of Ronneberger [RON 77], based only on the velocity profile of the turbulent flow, is in excellent agreement with measurement. Attempts could be made to use the approach of Ronneberger with respect to the determination of the Mach dependency in the theories including the effect of turbulent viscosity. Since his final result is rather complex, due to the complete radial coordinatesystem he uses, it could be worth wile to attempt to rewrite his theory in wall coordinates, neglecting the curvature of the wall.

Bibliography

[ABO 86] M. Åbom and H. Bodén
Influence of errors on the two-microphone method for measuring acoustic properties in ducts.
J. Acoust. Soc. Am. vol. 79, 541 (1986).

[ABO 88] M. Åbom and H. Bodén
Error analysis of two-microphone measurements in ducts with flow. J. Acoust. Soc. Am. vol. 83, 2429 (1988).

[BAL 92] W.G.E. v. Ballegooijen
Demping van akoestische golven in pijpen:
- ijking debietmeting
- meting demping.
Report Technical University Eindhoven, No R-1145-S. (1992)

[BOD 89] H. Bodén
Characterization of fluid machines as sources of fluid borne noise.
Doctoral Thesis Dept. Techn. Ac., Royal inst. of techn. Sweden.
Rep. No. TRITA-TAK-8906 ISSN 0280-2082.

[CRC] *CRC Handbook of chemistry and physics.*
CRC Press Florida.

[DAV 80] Davies
Measurement of plane wave acoustic fields in flow ducts.
J. Sound and Vibration (1980) 72(4), 539-542.

[DIS 78] J.H.M. Disselhorst
Acoustic resonances in open tubes.
Thesis Technical University Twente, sept. 1978.

[HIN 75] J.O. Hinze
Turbulence.
Mc Graw-Hill Book Company, second edition (1975).

[HOW 79] M.S. Howe
The interaction of sound with low Mach number wall turbulence, with application to sound propagation in turbulent pipe flow.
J. Fluid Mech. (1979) vol.94(4), 729-744.

[HOW 84] M.S. Howe
On the absorption of sound by turbulence and other hydrodynamic flows.
J. Appl. Math. (1984) 32, 187-209.

[HUI 92] F.J.J. Huijsmans
Reflection and damping of plane acoustic waves in pipes.
Graduation Thesis Technical University Eindhoven (1992), Rep. No. R-1145-A.

[ING 74] U. Ingard and V.K. Singhal
Sound attenuation in turbulent pipe flow. J. Acoust. Soc. Am. vol. 55, 535 (1974).

[KON 91] J.A. van de Konijnenberg
An experimental study on the acoustic reflection coefficient of open pipes at low Helmholtz numbers.
Graduation Thesis Technical University Eindhoven (1991), Rep. No. R-1119-A.

[KLI 90] S.J. Kline and N.H. Afgan
1988 Zoran Zarić Memorial Conference. On near wall turbulence.
Hemisphere Publishing Corporation (1990).

[KRI 92] P. Kriesels
The propagation of sound in a gas filled pipe.

Overview of basic theories available in literature.
Report Technical University Eindhoven, transport physics, (1992)

[LAI 90] Y.G. Lai and R.M.C. So
On near-wall turbulent flow modelling.
J. Fluid Mech. (1990) vol.221, 641-673.

[LIG 80] J. Lighthill
Waves in fluids
Cambridge University Press (1980).

[LOU 92] B. Louis and D. Isabey
Interaction of oscillatory and constant turbulent flows in airway-like tubes during impedance measurement.
J. Appl. Physiol. 14-04-1992.

[MUN 90] M.L. Munjal and A.G. Doige
The two-microphone method incorporating the effects of mean flow and acoustical damping.
J. Sound and Vibration (1990) 157, 135-139.

[PIE 89] A.D. Pierce
Acoustics: an introduction to its physical principles and applications.
Acoust. Soc. Am. and Am. Inst. of Physics (1989).

[REY 72] W.C. Reynolds and A.K.M.F. Hussain
The mechanics of an organized wave in turbulent shear flow, part 3. Theoretical models and comparison with experiment.
J. Fluid Mech. (1972) vol.54(2),263-288.

[RON 77] D. Ronneberger and C. Ahrens
Wall shear stress caused by small amplitude perturbations of turbulent boundary-layer flow: an experimental investigation.
J. Fluid Mech. (1977) vol.83, 433.

[RON 75] D. Ronneberger
Genaue Messung der Schalldämpfung und der Phasengeschwindigkeit in durchströmten Rohren im Hinblick auf die

Wechselwirkung zwischen Schall un Turbulenz.
Habilitationsschrift Mathematisch-Naturwissenschafliche Fakultät der Universität Göttingen (1975).

[RON 87] D. Ronneberger
Theoretische und experimentelle Untersuchung der Schallausbreitung durch Querschnittsprünge und Lochplatten in Strömungskanälen.
Drittes Physikalisches Institut der Universität Göttingen, (1987) Ro 669/11, 12, 14.

[SAV 71] S.D. Savkar
Propagation of sound in ducts with shear flow.
J. Sound and Vibration (1971) 19(3), 355-372.

[SHA 91] P. Shakkottai, E.Y. Kwack and L.H. Back.
Aero-acoustic flow sensor
Rev. Sci. Instr. (1991) 62(9), 2205-2212.

[SCH 79] Schlichting
Boundary-layer Theory
Mc Graw-Hill Book Company (1979).

[TIJ 75] H. Tijdeman
On the propagation of sound in cylindrical tubes.
J. Sound and Vibration 39(1), 1-33, also NLR report MP 74004 U.(1975)

List of symbols

a	pipe radius
$\mathcal{A}$	cross-sectional area
c, c_0	speed of sound, adiabatic
c_p, c_v	specific heat at constant pressure, volume
f	frequency
H_{ba}	transfer function from position a to position b
H_m^n	Hankel function of order n and kind m
i	$\sqrt{-1}$, index
k	complex wavenumber
K	Karmanns constant
$\mathcal{L}$	perimeter of cross-sectinal area $\mathcal{A}$
m_0	stationary local Mach number
M	stationary global Mach number
P, p	pressure
Pr, Pr_t	Prandtl number, turbulent
Re	Reynolds number
R	reflection coefficient
s	entropy
T	temperature
t	time
u	velocity in x-direction (axial)
u^*	friction velocity
$\vec{v} = (u, v, w)$	velocity
v	velocity in y-direction (radial, wall: $y = 0$)
x	axial coordinate
y	radial coordinate, normal to wall
z	wall impedance
Z	wall impedance, normalized with α_0

Greek

α, α_0, α_v	attenuation coefficient, quiescent case, quiescent case viscous part
β	coefficient of thermal expansion
γ	Poission ratio c_p/c_v
δ_l, δ_l^+	thickness of laminar sublayer of turbulent

	flow, dimensionless
$\delta_v,\ \delta_v^+$	thickness of viscous (acoustical) sublayer, dimensionless
$\delta_v,\ \delta_T^+$	thickness of thermal (acoustical) sublayer, dimensionless
$\eta,\ \eta_t$	dynamic viscosity, turbulent
$\kappa,\ \kappa_t$	heat conduction coefficient, turbulent
λ	wavelength
ν	order of Bessels equation
ρ	density
τ	shear stress
ω	radial frequency
ψ	friction factor
Φ	heat flow

super- and subscripted

Q_{ac}	acoustical contribution
Q_{bl}	boundary-layer contribution
Q_0	quantity evaluated at $y = 0$; static value
Q_v	viscous part
Q_T	thermal part
Q_t	turbulent
$Q_\pm$	up- and downstream value
Q^+	made dimensionless with $\eta/\rho_0 u^*$
Q'	acoustical deviation from static quantity
$\tilde{Q}$	turbulent deviation from static quantity
$\overline{Q}$	average
$\hat{Q}$	complex amplitude
$\|Q\|$	norm of complex quantity
$\phi(Q)$	angle of complex quantity
$\Re(Q)$	real part
$\Im(Q)$	imaginairy part

$\frac{\partial}{\partial x}$	partial derivative in x-direction

$\frac{D}{Dt} = \frac{\partial}{\partial t} + u_0 \frac{\partial}{\partial x}$ convective time derivative (total derivative)